

## **General Disclaimer**

### **One or more of the Following Statements may affect this Document**

- This document has been reproduced from the best copy furnished by the organizational source. It is being released in the interest of making available as much information as possible.
- This document may contain data, which exceeds the sheet parameters. It was furnished in this condition by the organizational source and is the best copy available.
- This document may contain tone-on-tone or color graphs, charts and/or pictures, which have been reproduced in black and white.
- This document is paginated as submitted by the original source.
- Portions of this document are not fully legible due to the historical nature of some of the material. However, it is the best reproduction available from the original submission.

ELECTROMAGNETICS LABORATORY  
TECHNICAL REPORT NO. 85-8

September 1985

NORMAL MODES IN AN OVERMODED CIRCULAR WAVEGUIDE  
COATED WITH LOSSY MATERIAL

C. S. Lee  
S. W. Lee  
S. L. Chuang

Supported by  
Grant NAG3-475  
NASA-Lewis Research Center  
Cleveland, Ohio 44135



ELECTROMAGNETICS LABORATORY  
DEPARTMENT OF ELECTRICAL AND COMPUTER ENGINEERING  
ENGINEERING EXPERIMENT STATION  
UNIVERSITY OF ILLINOIS AT URBANA-CHAMPAIGN  
URBANA, ILLINOIS 61801

(NASA-CR-176186) NORMAL MODES IN AN  
OVERMODED CIRCULAR WAVEGUIDE COATED WITH  
LOSSY MATERIAL (Illinois Univ.) 55 P  
HC A04/MF A01

CSCL 20N

G3/32

N85-35320

Unclass

27415

Electromagnetics Laboratory Report No. 85-8

NORMAL MODES IN AN OVERMODED CIRCULAR WAVEGUIDE  
COATED WITH LOSSY MATERIAL

by

C. S. Lee, S. W. Lee and S. L. Chuang

Technical Report

September 1985

Supported by

Grant No. NAG3-475  
NASA-Lewis Research Center  
Cleveland, Ohio 44135

Electromagnetics Laboratory  
Department of Electrical and Computer Engineering  
Engineering Experiment Station  
University of Illinois at Urbana-Champaign  
Urbana, Illinois 61801

# TABLE OF CONTENTS

	Page
I. INTRODUCTION . . . . .	2
II. OVERVIEW OF MODAL FIELDS IN A COATED CIRCULAR WAVEGUIDE . . . . .	3
A. Mode Classification . . . . .	3
B. Cutoff Frequencies . . . . .	4
C. Modal Propagation Constant and Power Distribution . . . . .	5
D. Transverse-field Distribution . . . . .	6
III. MODAL CHARACTERISTIC EQUATIONS, FIELDS AND CLASSIFICATION . . . . .	7
A. Inner Mode . . . . .	10
B. Surface Mode . . . . .	12
C. Interface Mode . . . . .	14
IV. NUMERICAL RESULTS AND DISCUSSION . . . . .	16
A. Lossless Coating . . . . .	16
B. Slightly Lossy Coating . . . . .	16
C. Very Lossy Coating . . . . .	17
D. Mode Suppressor . . . . .	19
E. CP Antenna . . . . .	19
V. CONCLUSION . . . . .	20
REFERENCES . . . . .	20
APPENDIX 1. DEGENERACY BETWEEN THE CUTOFF FREQUENCIES OF THE $TM_{11}$ and $TE_{01}$ MODES IN A DIELECTRIC-COATED CIRCULAR WAVEGUIDE . . .	22
APPENDIX 2. FIELDS OF THE NORMAL MODES IN A COATED CIRCULAR GUIDE WHEN $k_{p1} = 0$ . (DIRECT METHOD). . . . .	24
FIGURES . . . . .	29

# LIST OF FIGURES

Figure		Page
1.	A coated circular waveguide. . . . .	29
2.	The cutoff frequencies in a dielectric-coated waveguide ( $\epsilon_2 = 10$ , $\mu_2 = 1$ ) normalized to that of the $TE_{11}$ mode in an empty guide ( $f_{co}$ ) as a function of coating thickness. . . . .	30
3.	The cutoff frequencies in a magnetic-coated waveguide ( $\mu_2 = 10$ , $\epsilon_2 = 1$ ) normalized to that of the $TE_{11}$ mode in an empty guide ( $f_{co}$ ) as a function of coating thickness. . . . .	31
4.	Mode transition in a coated circular guide at the high-frequency limit. The $HE_{mn}$ modes approach modes in a PMC-PEC guide, and the $EH_{mn}$ approach modes in PEC-PEC guide. . . . .	32
5.	a) Normalized propagation constant and b) radial wave number ( $k_{\rho 1}a$ ) of the $HE_{11}$ mode in a dielectric-coated waveguide ( $\epsilon_2 = 10$ , $\mu_2 = 1$ ) as a function of the coating thickness in "effective" wavelength ( $\tau' = \tau\sqrt{\epsilon_2\mu_2/\lambda}$ ). The power distributions for the four marked points are shown in Figure 6. The approximate solution of the surface mode using the two-slab model is also shown (see Section III) . . . .	33
6.	Normalized angle-averaged power distribution in watts/ $\lambda^2$ as a function of radial distance in a dielectric-coated waveguide ( $\epsilon_2 = 10$ , $\mu_2 = 1$ ) with four different coating thicknesses. The corresponding points for these diagrams are marked in Figure 5 ( $\tau' = \tau\sqrt{\epsilon_2\mu_2/\lambda}$ ) . . . . .	34
7.	a) Normalized propagation constant and b) radial wave number ( $k_{\rho 1}a$ ) of the $HE_{11}$ mode in a magnetic-coated waveguide ( $\mu_2 = 10$ , $\epsilon_2 = 1$ ) as a function of the lining thickness in "effective" wavelength ( $\tau' = \tau\sqrt{\epsilon_2\mu_2/\lambda}$ ). The power distributions of the four marked points are shown in Figure 8. The approximate solution of the surface mode using the two-slab model is also shown (see Section III) . . . .	35
8.	Normalized angle-averaged power distribution in watts/ $\lambda^2$ as a function of radial distance in a magnetic-coated waveguide ( $\mu_2 = 10$ , $\epsilon_2 = 1$ ) with four different coating thicknesses. The corresponding points for these diagrams are marked in Figure 7 ( $\tau' = \tau\sqrt{\epsilon_2\mu_2/\lambda}$ ) . . . . .	36
9.	Transverse field distributions of the normal modes in a) empty guide, b) dielectric-coated guide at cutoff frequencies, c) magnetic-coated guide at cutoff frequencies and d) coated guide at the high-frequency limit. . . . .	37

Figure		Page
10.	Radial wave numbers of the normal modes in a waveguide coated with lossless dielectric material ( $\epsilon_2 = 10, \mu_2 = 1, a/\lambda = 3.33$ ). . . . .	38
11.	Radial wave numbers of the normal modes in a waveguide coated with a lossless magnetic material ( $\mu_2 = 10, \epsilon_2 = 1, a/\lambda = 3.33$ ). . . . .	39
12.	Radial wave numbers of the normal modes in a circular waveguide coated with a lossy dielectric material ( $\epsilon_2 = \exp(-j\phi_e), \phi_e = 5^\circ, \mu_r = 1, a/\lambda = 3.33$ ). . . . .	40
13.	Radial wave numbers of the normal modes in a circular waveguide coated with a lossy magnetic material ( $\mu_2 = \exp(-j\phi_m), \phi_m = 5^\circ, \epsilon_2 = 1, a/\lambda = 3.33$ ). . . . .	41
14.	Attenuation constants of the normal modes in a circular waveguide coated with a lossy dielectric material ( $\epsilon_2 = \exp(-j\phi_e), \phi_e = 5^\circ, \mu_r = 1, a/\lambda = 3.33$ ). . . . .	42
15.	Attenuation constants of the normal modes in a circular waveguide coated with a lossy magnetic material ( $\mu_2 = \exp(-j\phi_m), \phi_m = 5^\circ, \epsilon_2 = 1, a/\lambda = 3.33$ ). . . . .	43
16.	Radial wave numbers of the normal modes in a circular waveguide coated with a lossy dielectric material ( $\epsilon_2 = \exp(-j\phi_e), \phi_e = 45^\circ, \mu_2 = 1, a/\lambda = 3.33$ ). . . . .	44
17.	Radial wave numbers of the normal modes in a circular waveguide coated with a lossy magnetic material ( $\mu_2 = \exp(-j\phi_m), \phi_m = 45^\circ, \epsilon_2 = 1, a/\lambda = 3.33$ ). . . . .	45
18.	Attenuation constants of the normal modes in a circular waveguide coated with a lossy dielectric material ( $\epsilon_2 = \exp(-j\phi_e), \phi_e = 45^\circ, \mu_2 = 1, a/\lambda = 3.33$ ). . . . .	46
19.	Attenuation constants of the normal modes in a circular waveguide coated with a lossy magnetic material ( $\mu_2 = \exp(-j\phi_m), \phi_m = 45^\circ, \epsilon_2 = 1, a/\lambda = 3.33$ ). . . . .	47
20.	Attenuation constants of the normal modes as a function of the inner radius, $a$ , with a fixed layer thickness ( $\tau = 0.949 \lambda / \sqrt{ \epsilon_2 \mu_2 }$ ) in a circular waveguide coated with a lossy dielectric material ( $\epsilon_2 = \exp(-j\phi_e), \phi_e = 45^\circ, \mu_2 = 1, a_0/\lambda = 3.33$ ). The mode names in the parentheses correspond to those in Marcatili and Schmeltzer's paper [5]. . .	48

21. Attenuation constants of the normal modes as a function of the inner radius,  $a$ , with a fixed layer thickness ( $\tau = 0.949 \lambda / \sqrt{\epsilon_2 \mu_2}$ ) in a circular waveguide coated with a lossy magnetic material ( $\mu_2 = \exp(-i\phi_m)$ ,  $\phi_m = 45^\circ$ ,  $\epsilon_2 = 1$ ,  $a_0/\lambda = 3.33$ ). The mode names in the parentheses correspond to those in Marcatili and Schmeltzer's paper [5]. . . 49

# ABSTRACT

The normal modes in an overmoded waveguide coated with a lossy material are analyzed, particularly for their attenuation properties as a function of coating material, layer thickness, and frequency. When the coating material is not too lossy, the low-order modes are highly attenuated even with a thin layer of coating. This coated guide serves as a mode suppressor of the low-order modes, which can be particularly useful for reducing the radar cross section (RCS) of a cavity structure such as a jet engine inlet. When the coating material is very lossy, low-order modes fall into two distinct groups: highly and lowly attenuated modes. However, as  $a/\lambda$  ( $a$  = radius of the cylinder;  $\lambda$  = the free-space wavelength) increases, the separation between these two groups becomes less distinctive. The attenuation constants of most of the low-order modes become small, and decrease as a function of  $\lambda^2/a^3$ .



## I. INTRODUCTION

In many applications, it is desirable to line the wall of a conventional circular waveguide by a layer of dielectric or magnetic material. With proper design, the lining can significantly alter the modal fields in the waveguide, so as to achieve either less attenuation or more attenuation for certain modes. The past studies of this problem are mostly connected with microwave/infrared transmission over a long distance [1] - [5]. Two assumptions are usually made:

- (1) The waveguide diameter is very large in terms of wavelength (overmoded waveguide); and
- (2) The coating material is either nearly lossless [2] - [4] or very lossy [5].

These assumptions simplify the theoretical analysis and oftentimes bring out a clearer physical picture. Nevertheless, in many practical situations, these assumptions are too restrictive. A more general analysis of the coated circular waveguide is needed.

It is the purpose of this paper to fill in this need. Instead of using the perturbation theory [2], [3], [5], transmission-line model [1] - [4] or asymptotic theory [6], we solve the modal characteristic equation of a coated circular waveguide exactly by a numerical method. This is feasible because of today's fast computers and efficient subroutines for calculating Bessel functions with a complex argument.

The organization of the paper is as follows: First, an overview of the normal modes in a coated circular waveguide in comparison with those in an uncoated waveguide is presented. In Section III, the exact characteristic equation for the normal modes in a circular waveguide coated with a lossy

material is given. Three types of normal modes, i.e., the inner mode, the surface mode and the interface mode, are discussed, along with their approximate solutions. Numerical results and potential applications are discussed in Section IV.

## II. OVERVIEW OF MODAL FIELDS IN A COATED CIRCULAR WAVEGUIDE

Before presenting detailed numerical results, it is beneficial to explain some unique features of the coated waveguide, which are absent in the conventional uncoated waveguide. Figure 1 shows a circular waveguide with a perfectly conducting wall, uniformly coated with a material of permittivity  $\epsilon_2\epsilon_0$  and permeability  $\mu_2\mu_0$ . Both  $\epsilon_2$  and  $\mu_2$  can be complex, with their negative imaginary parts representing material losses for the present  $\exp(j\omega t)$  time convention. The medium in Region I is assumed to be air, i.e., permittivity  $\epsilon_0$  and permeability  $\mu_0$ . Our problem at hand is to study the normal modes in such a waveguide.

### A. Mode Classification

In an uncoated waveguide, the normal modes are either TE or TM with respect to  $z$ . Here index  $m$  describes the azimuthal variation in the form of  $\sin m\phi$  or  $\cos m\phi$ , whereas index  $n$  describes the radial distribution in the form of  $J_m(k_{\rho n}\rho)$  or  $J'_m(k_{\rho n}\rho)$ . In the ascending order of their cutoff frequencies, the dominant modes are

$$TE_{11}, TM_{01}, TE_{21}, TM_{11}/TE_{01}, \dots$$

When the waveguide is coated with a dielectric layer, there are no longer pure TE or TM modes. The modes are commonly classified into  $HE_{mn}$  and  $EH_{mn}$  modes in such a way that, in the limiting case of a vanishingly thin coating [7],

$$HE_{mn} \rightarrow TE_{mn}, \quad \text{and} \quad EH_{mn} \rightarrow TM_{mn}$$

There exist three special cases where  $HE_{mn}$  ( $EH_{mn}$ ) becomes identically or approximately  $TE_{mn}$  ( $TM_{mn}$ ), namely,

- (i) circularly symmetrical modes ( $m = 0$ ) such as  $TE_{0n}$  and  $TM_{0n}$ ,
- (ii) all modes at frequencies near their cutoff frequencies [8], [9],  
and
- (iii) the low-order modes in an overmoded waveguide coated with a lossless material, (in this limit  $HE_{mn} \rightarrow TM_{mn}$ , and  $EH_{mn} \rightarrow TE_{mn}$ ).

#### B. Cutoff Frequencies

Near the cutoff frequency, the normal mode is either quasi TE or TM. In Figures 2 and 3, we plot the cutoff frequencies  $f_c$ 's of the normal modes in a coated circular guide as a function of layer thickness  $\tau$ .  $f_c$  is normalized with respect to  $f_{co}$ , which is the cutoff frequency of the dominant  $TE_{11}$  mode in an empty guide of radius  $a$ , and is given by

$$f_{co} = \frac{1.84118 c}{2\pi a}$$

where  $c$  is the speed of light in free space. Figure 2 shows the modal inversion between the  $TM_{01}$  and  $TE_{21}$ , which has been previously reported [8], [9]. However, the modal inversion between those two modes is not evident if the coating is of a magnetic material ( $\mu_2 \neq 1$ ) instead of a dielectric material (Figure 3). Coating reduces the cutoff frequencies of the normal modes, especially for the magnetic-coated waveguide. This is due to the fact that, with coating, the modal field distribution tends to concentrate near the air-material interface. Note also that the degeneracy between the  $TM_{11}$  and  $TE_{01}$  modes near their cutoff frequencies is not removed by the dielectric coating (see Appendix 1), but the degeneracy can be removed by the magnetic coating. The near degeneracy of the  $TE_{01}$  mode with the  $TM_{11}$  mode in a dielectric-coated guide can

cause a serious problem for a long-distance communication utilizing the lowly attenuating  $TE_{01}$  mode because there may be a large mode conversion due to a strong coupling between these two modes [2] - [4]. The magnetic coating can be very useful in this application.

### C. Modal Propagation Constant and Power Distribution

When the coating thickness is small in terms of the free-space wavelength ( $\tau/\lambda \ll 1$ ), the modal field distribution in the air region and the propagation constant are not much perturbed. As the coating thickness is increased in the manner

$$\tau/\lambda \rightarrow \infty, \text{ for a fixed value of } a$$

the low-order modes approach, one by one, their counterparts in the parallel-plate waveguide. More precisely, the  $HE_{mn}$  modes in a coated circular waveguide approach those modes in a parallel-plate waveguide formed by a perfect magnetic conductor (PMC) and perfect electric conductor (PEC) as sketched in Figure 4a. The  $EH_{mn}$  modes approach those modes in a parallel-plate waveguide formed by two PEC's as shown in Figure 4b.

The propagation constant  $k_z$  and modal power distribution of the dominant  $HE_{11}$  mode in a guide coated with a lossless dielectric material ( $\epsilon_2 = 10$ ,  $\mu_2 = 1$ ) are shown in Figures 5 and 6. When the coating thickness is small ( $\tau'/\lambda = \tau/\lambda_2 < 0.05$ , where  $\lambda_2 = \lambda/\sqrt{\epsilon_2\mu_2}$  = wavelength in Region II), the transverse wave number  $k_{\rho 1}$  in Region I defined by

$$k_{\rho 1} = \sqrt{k_0^2 - k_z^2}$$

is real, where  $k_0 = 2\pi/\lambda$ , and both propagation constant and its power-intensity distribution are very similar to those of an empty guide. When the coating thickness  $\tau$  is much larger than  $0.05 \lambda_2$ ,  $k_{\rho 1}$  is imaginary and its magnitude

approaches  $k_0\sqrt{\epsilon_2\mu_2} - 1$ . Consequently, the modal power distribution is largely concentrated in the dielectric layer (Region II). In Figure 6, the total power carried by the  $HE_{11}$  mode is normalized to 1 watt. In case (4) of Figure 6, more than 99% of the power is confined in the dielectric layer, despite the fact that the dielectric layer ( $1.06 < \rho/a < 1$ ) covers only 12% of the waveguide cross section.

Figures 7 and 8 are similar to Figures 5 and 6 except that the coating material is magnetic ( $\mu_2 = 10$  and  $\epsilon_2 = 1$ ). It is most interesting to observe that the transition point where  $k_z$  becomes imaginary occurs at a much smaller coating thickness ( $\tau = 0.05 \lambda_2$  in Figure 5 and  $\tau = 0.005 \lambda_2$  in Figure 7). Thus, in applications where large field concentration in the material layer is desired, the magnetic coating is more effective (more discussion is given in Section IV).

It is worthwhile to note that the normal mode at the transition point is not TEM even though the radial wave number vanishes (see Appendix 2). Thus, both the hybrid-mode method and the techniques for TEM modes fail to provide the modal fields at the transition point. Only the direct method as discussed in Appendix 2 is applicable in this case.

#### D. Transverse-field Distribution

The transverse fields of the five lowest-order modes in an uncoated circular guide and in a coated (dielectric and magnetic) circular guide at the cutoff frequencies and the high-frequency limits are shown in Figure 9. The TE (TM) modes in a circular guide at the cutoff frequencies do not have transverse magnetic (electric) fields, which are not shown in the diagrams. We notice that the nonvanishing fields at the cutoff frequencies are similar to those in an uncoated guide. At high frequency, the fields are confined within the coated

region, as shown in the diagrams where the blank space indicates that the fields are negligible.

### III. MODAL CHARACTERISTIC EQUATIONS, FIELDS AND CLASSIFICATION

The general problem is shown in Figure 1. Here both the permittivity  $\epsilon_2\epsilon_0$  and permeability  $\mu_2\mu_0$  of the coating material are allowed to be complex. The characteristic equation for the propagation constant  $k_z$  of a normal mode is well known [10], [11], and we list the final expression, which is solved numerically using Müller's method (available in International Mathematical Statistical Libraries subroutines):

$$k_{\rho 1}^2 \left[ F_1'(a) - \epsilon_2 \frac{F_1(a)F_3'(a)}{F_3(a)} \frac{k_{\rho 1}}{k_{\rho 2}} \right] \left[ F_1'(a) - \mu_2 \frac{F_1(a)F_4'(a)}{F_4(a)} \frac{k_{\rho 1}}{k_{\rho 2}} \right] - [k_{zm}/(k_0 a)]^2 F_1^2(a) [1 - (k_{\rho 1}/k_{\rho 2})^2]^2 = 0 \quad (1a)$$

where

$$k_{\rho 1}^2 + k_z^2 = k_0^2 \quad (1b)$$

$$k_{\rho 2}^2 + k_z^2 = \epsilon_2 \mu_2 k_0^2 \quad (1c)$$

$$F_1(\rho) = J_m(k_{\rho 1} \rho), \quad F_1'(\rho) = J_m'(k_{\rho 1} \rho) \quad (1d)$$

$$F_3(\rho) = J_m(k_{\rho 2} \rho) N_m(k_{\rho 2} b) - N_m(k_{\rho 2} \rho) J_m(k_{\rho 2} b) \quad (1e)$$

$$F_3'(\rho) = J_m'(k_{\rho 2} \rho) N_m(k_{\rho 2} b) - N_m'(k_{\rho 2} \rho) J_m(k_{\rho 2} b) \quad (1f)$$

$$F_4(\rho) = J_m(k_{\rho 2} \rho) N_m'(k_{\rho 2} b) - N_m(k_{\rho 2} \rho) J_m'(k_{\rho 2} b) \quad (1g)$$

$$F_4'(\rho) = J_m'(k_{\rho 2} \rho) N_m'(k_{\rho 2} b) - N_m'(k_{\rho 2} \rho) J_m'(k_{\rho 2} b) \quad (1h)$$

Here  $k_{\rho 1}$  and  $k_{\rho 2}$  are the radial wave vectors of regions I and II, respectively;  $\omega$  is the angular frequency;  $k_0 = 2\pi/\lambda$ ; and  $a$  and  $b$  are the radii of the air region and the conducting cylinder, respectively.  $J_m$  is the Bessel function and  $N_m$  is the Neumann function of order  $m$ . The prime indicates differentiation with respect to argument. The modal fields are given by

$$E_{\rho}^I = -[(Ak_z/k_0) F_1'(\rho) + (Bm/k_{\rho 1}\rho) F_1(\rho)] \cos m\phi \quad (2a)$$

$$E_{\rho}^{II} = -[(Ck_z/k_2) F_3'(\rho) + (Dm/k_{\rho 2}\rho) F_4(\rho)] \cos m\phi \quad (2b)$$

$$E_{\phi}^I = [\{Ak_z m/(k_0 k_{\rho 1}\rho)\} F_1(\rho) + BF_1'(\rho)] \sin m\phi \quad (2c)$$

$$E_{\phi}^{II} = [\{Ck_z m/(k_2 k_{\rho 2}\rho)\} F_3(\rho) + DF_4'(\rho)] \sin m\phi \quad (2d)$$

$$E_z^I = -j(Ak_{\rho 1}/k_0) F_1(\rho) \cos m\phi \quad (2e)$$

$$E_z^{II} = -j(Ck_{\rho 2}/k_2) F_3(\rho) \cos m\phi \quad (2f)$$

$$H_{\rho}^I = -Y_0[(Am/k_{\rho 1}\rho) F_1(\rho) + (Bk_z/k_0) F_1'(\rho)] \sin m\phi \quad (2g)$$

$$H_{\rho}^{II} = -Y_2[(Cm/k_{\rho 2}\rho) F_3(\rho) + (Dk_z/k_2) F_4'(\rho)] \sin m\phi \quad (2h)$$

$$H_{\phi}^I = -Y_0[F_1'(\rho) + \{Bk_z m/(k_0 k_{\rho 1}\rho)\} F_1(\rho)] \cos m\phi \quad (2i)$$

$$H_{\phi}^{II} = -Y_2[CF_3'(\rho) + \{Dk_z m/(k_2 k_{\rho 2}\rho)\} F_4(\rho)] \cos m\phi \quad (2j)$$

$$H_z^I = -jY_0(Bk_{\rho 1}/k_0) F_1(\rho) \sin m\phi \quad (2k)$$

$$H_z^{II} = -jY_2(Dk_{\rho 2}/k_2) F_4(\rho) \sin m\phi \quad (2l)$$

The convention of  $\exp[j(\omega t - k_z z)]$  is understood and omitted; superscripts I and II indicate Regions I and II (Figure 1), and subscripts  $\rho$ ,  $\phi$  and  $z$  indicate the radial, angular and propagation-directional components of the fields,

respectively;  $k_2 = \sqrt{\epsilon_2 \mu_2} k_0$ ; and  $Y_0$  is the free-space admittance,  $\sqrt{\epsilon_0/\mu_0}$  and  $Y_2 = Y_0 \sqrt{\epsilon_2/\mu_2}$ . A, B, C and D are the constants, which are determined by the boundary conditions and the normalization requirement. Those constants are related by

$$C = A \sqrt{\epsilon_2 \mu_2} k_{\rho 1} F_1(a) / [k_{\rho 2} F_3(a)] \quad (3)$$

$$D = B \mu_2 k_{\rho 1} F_1(a) / [k_{\rho 2} F_4(a)] \quad (4)$$

$$\frac{B}{A} = - \frac{k_0 k_{\rho 1} a [F_1'(a)/F_1(a) - \epsilon_2 k_{\rho 1} F_3'(a) / \{k_{\rho 2} F_3(a)\}]}{k_{zm} [1 - (k_{\rho 1}/k_{\rho 2})^2]} \quad (m \neq 0) \quad (5)$$

$$(|\frac{B}{A}| \ll 1 \text{ for "quasi" TM modes})$$

Equation (5) can also be written as

$$\frac{A}{B} = - \frac{k_0 k_{\rho 1} a [F_1'(a)/F_1(a) - \mu_2 k_{\rho 1} F_4'(a) / \{k_{\rho 2} F_4(a)\}]}{k_{zm} [1 - (k_{\rho 1}/k_{\rho 2})^2]} \quad (m \neq 0) \quad (6)$$

$$(|\frac{A}{B}| \ll 1 \text{ for "quasi" TE modes})$$

and the elimination of A and B from Eqs. (5) and (6) gives the characteristic equation (Eq. (1)). There is no mode coupling between the TE and TM modes for  $m = 0$ . Thus,  $A = 0$  and  $B = 1$  for the  $TM_{0n}$  modes, and  $A = 1$  and  $B = 0$  for the  $TE_{0n}$  modes. We note that there are two degenerate modes for each angular mode index  $m$  except  $m = 0$ . In the above expression of the fields, we have arbitrarily chosen one of those two modes.

There are three types of normal modes in an overmoded waveguide coated with a lossy material. The properties of these modes are explained below along with the approximate propagation constants and field distributions.



#### A. Inner Mode

When the coating material is sufficiently lossy and  $a/\lambda$  is large, most of the low-order modes become inner modes. The field distributions of these modes are mostly confined in the air region. In the limit as  $a/\lambda$  becomes infinite, the characteristic equation is simplified to

$$[F_1'(a)/F_1(a)]^2 - (m/x)^2 = 0 \quad (7)$$

where

$$x = k_{p1}a$$

The solutions of this equation are

$$J_{m-1}(x_0^+) = 0 \quad \text{for} \quad EH_{mn}^{MS} \quad (8)$$

$$J_{m+1}(x_0^-) = 0 \quad \text{for} \quad EH_{-mn}^{MS} \quad (9)$$

Superscript MS indicates the notation by Marcatili and Schmeltzer. This superscript is used to distinguish this notation from the conventional notation. In this case, the field distributions are also simplified. Equations (6) (or equivalently Eq. (5)) in this limit becomes

$$A/B = +1 \quad \text{for} \quad EH_{mn}^{MS} \quad (10)$$

$$A/B = -1 \quad \text{for} \quad EH_{-mn}^{MS} \quad (11)$$

and the modal fields in the air region are given by

$$E_\rho = -BJ_{m-1}(k_{\rho 0}^+ \rho) \cos m\phi, \quad H_\rho = -Y_0 E_\phi \quad (12a)$$

$$E_\phi = BJ_{m-1}(k_{\rho 0}^+ \rho) \sin m\phi, \quad H_\phi = Y_0 E_\rho \quad (12b)$$

$$E_z = H_z = 0 \quad \text{for } EH_{mn}^{MS} \quad (12c)$$

$$E_\rho = -BJ_{m+1}(k_{\rho 0}^- \rho) \cos m\phi, \quad H_\rho = -Y_0 E_\phi \quad (13a)$$

$$E_\phi = -BJ_{m+1}(k_{\rho 0}^- \rho) \sin m\phi, \quad H_\phi = Y_0 E_\rho \quad (13b)$$

$$E_z = H_z = 0 \quad \text{for } EH_{-mn}^{MS} \quad (13c)$$

where

$$k_{\rho 0}^+ = x_0^+/a, \quad k_{\rho 0}^- = x_0^-/a$$

Here  $x_0^+$  and  $x_0^-$  are given in Eqs. (8) and (9), respectively, and B is a constant. The fields in the lossy region are vanishingly small. The field diagrams of the  $EH_{mn}^{MS}$  and  $EH_{-mn}^{MS}$  modes in the air region are shown in Figure 2 in Reference [2].

When  $a/\lambda$  is large but finite, the attenuation constants of the normal modes are small and the fields decay very rapidly from the interface to the lossy layer. In this case, the asymptotic forms of the Bessel functions can be used for the field functions in the lossy region. The characteristic function of Eq. (1) in this approximation is then simplified to

$$\begin{aligned} & [xF_1'(a)/F_1(a)]^2 + jx[xF_1'(a)/F_1(a)](k_{\rho 1}/k_{\rho 2})(\epsilon_2 + \mu_2) \\ & - m^2 - x^2 \epsilon_2 \mu_2 (k_{\rho 1}/k_{\rho 2})^2 = 0 \end{aligned} \quad (14)$$

where  $x = k_{\rho 1} a$

Suppose  $x = x_0 + \Delta x$  where  $x_0$  is the solution as  $a/\lambda$  becomes infinite. Taking the first-order terms in  $k_{\rho 1}/k_{\rho 2}$  of the above equation, the attenuation constant is given by

$$\alpha_{mn} = \left( \frac{\xi_{mn}}{2\pi} \right)^2 \frac{\lambda^2}{a^3} \operatorname{Re}(v_n) \quad (15a)$$

where

$$v_n = \begin{cases} \epsilon_2 / \sqrt{\epsilon_2 \mu_2 - 1} & \text{for } \text{TM}_{0n} \text{ modes } (m = 0) \\ \mu_2 / \sqrt{\epsilon_2 \mu_2 - 1} & \text{for } \text{TE}_{0n} \text{ modes } (m = 0) \\ \frac{1}{2} (\epsilon_2 + \mu_2) / \sqrt{\epsilon_2 \mu_2 - 1} & \text{for } \text{EH}_{mn}^{\text{MS}} \text{ and } \text{EH}_{-mn}^{\text{MS}} (m \neq 0) \end{cases} \quad (15b)$$

$$(15c)$$

$$(15d)$$

Here  $\xi_{mn}$  is the solution of

$$J_0'(\xi_{0n}) = 0 \quad \text{for } \text{TM}_{0n} \text{ and } \text{TE}_{0n} \text{ modes } (m = 0) \quad (15e)$$

$$J_{m-1}(\xi_{mn}) = 0 \quad \text{for } \text{EH}_{mn}^{\text{MS}} \text{ modes } (m \neq 0) \quad (15f)$$

$$J_{m+1}(\xi_{mn}) = 0 \quad \text{for } \text{EH}_{-mn}^{\text{MS}} \text{ modes } (m \neq 0) \quad (15g)$$

This is almost the same as the result of Marcatili and Schmeltzer except that the coating material is not restricted to a dielectric but can be magnetic as well.

For the first-order approximation of the attenuation constant with  $m \neq 0$ , we neglected the last term of Eq. (14). Even though this term is of the second order in  $k_{\rho 1}/k_{\rho 2}$ , the coefficient  $|x^2 \epsilon_2 \mu_2|$  can be a large number for the higher-order modes. Thus we expect that the agreement between our exact solution and the first-order solution requires a larger value of  $a/\lambda$  for a higher-order mode (more discussion is given in Section IV).

#### B. Surface Mode

When the coating material is not lossy enough, some of the normal modes become surface modes. The fields of those modes are confined within the thin

layer of the coating and the propagation constants are nearly independent of the inner radius  $a$ . When  $a/\lambda$  is sufficiently large, the characteristic equation is approximated to

$$\left[1 + \epsilon_2 \frac{jk_{\rho 1}}{k_{\rho 2}} \cot(k_{\rho 2} \tau)\right] \left[1 - \mu_2 \frac{jk_{\rho 1}}{k_{\rho 2}} \tan(k_{\rho 2} \tau)\right] = 0 \quad (16)$$

where  $\tau$  is the layer thickness,  $b - a$ . Assuming  $|k_{\rho 1}| \gg k_0$ , we obtain

$$k_z = \begin{cases} [\epsilon_2 \mu_2 k_0^2 - \{(n - \frac{1}{2}) \pi / \tau\}^2]^{1/2} & \text{for } TM_{mn}^{su} \\ [\epsilon_2 \mu_2 k_0^2 - (n\pi / \tau)^2]^{1/2} & \text{for } TE_{mn}^{su} \end{cases} \quad (17)$$

$$\quad \quad \quad (18)$$

where  $n = 1, 2, 3, \dots$

Superscript  $su$  indicates the surface mode. The fields in Region II in this limit can be approximately shown to be

$$E_\rho = C_1 \cos k_{\rho 2}(b - \rho) \quad (19a)$$

$$E_z = -jC_1(k_{\rho 2}/k_z) \sin k_{\rho 2}(b - \rho) \quad (19b)$$

$$H_\phi = C_1 Y_2(k_z/k_2) \cos k_{\rho 2}(b - \rho) \quad (19c)$$

$$E_\phi = H_\rho = H_z = 0 \quad \text{for } TM_{mn}^{su} \quad (19d)$$

$$E_\phi = D_1 \sin k_{\rho 2}(b - \rho) \quad (20a)$$

$$H_\rho = -D_1 Y_2(k_z/k_2) \sin k_{\rho 2}(b - \rho) \quad (20b)$$

$$H_z = -jD_1 Y_2(k_{\rho 2}/k_2) \cos k_{\rho 2}(b - \rho) \quad (20c)$$

$$E_\rho = E_z = H_\phi = 0 \quad \text{for } TE_{mn}^{su} \quad (20d)$$

where  $C_1$  and  $D_1$  are constants. Thus the  $TE_{mn}^{su}$  mode can be approximated by a normal mode between two PEC slabs and the  $TM_{mn}^{su}$  mode by a normal mode between PMC and PEC slabs. The correspondence between the normal modes in a thinly coated waveguide and the surface modes is not unique but depends on the type of coating material. When the coating material is lossless, the  $HE_{mn}(EH_{mn})$  modes become  $TM_{mn}^{su}(TE_{mn}^{su})$  (except  $m = 0$ ) as the layer thickness increases. The normal modes with  $m = 0$  are pure TE or TM as indicated in Section II.

### C. Interface Mode

There exists an "interface" mode, which is unique to the waveguide coated with a lossy material. The interface mode has large fields near the interface between the air and lossy regions, and the fields decay exponentially to both sides of the interface. Since the fields are limited to the interface region, the attenuation constant is independent of the radius of the waveguide. As  $a/\lambda$  is sufficiently large and the coating material is sufficiently lossy, the characteristic equation for the interface mode is well-approximated to

$$(1 + \epsilon_2 k_{\rho 1}/k_{\rho 2})(1 + \mu_2 k_{\rho 1}/k_{\rho 2}) = 0 \quad (21)$$

The propagation constants are then evaluated to be

$$k_z = \begin{cases} k_0 [(\epsilon_2^2 - \epsilon_2 \mu_2)/(\epsilon_2^2 - 1)]^{1/2} & \text{for } TM^{in} \\ k_0 [(\mu_2^2 - \epsilon_2 \mu_2)/(\mu_2^2 - 1)]^{1/2} & \text{for } TE^{in} \end{cases} \quad (22)$$

$$(23)$$

The modal fields are given by

$$E_{\rho}^I = C_2 \exp[jk_{\rho 1}(a - \rho)] , \quad E_{\rho}^{II} = (C_2/\epsilon_2) \exp[-jk_{\rho 2}(\rho - a)] \quad (24a)$$

$$E_z^I = -(k_{\rho 1}/k_z) E_{\rho}^I , \quad E_z^{II} = -(k_{\rho 2}/k_z) E_{\rho}^{II} \quad (24b)$$

$$H_{\phi}^I = (Y_0 k_0 / k_z) E_{\rho}^I, \quad H_{\phi}^{II} = (Y_2 k_2 / k_z) E_{\rho}^{II} \quad (24c)$$

for  $TM^{in}$

$$E_{\phi}^I = D_2 \exp[jk_{\rho 1}(a - \rho)], \quad E_{\phi}^{II} = D_2 \exp[-jk_{\rho 2}(\rho - a)] \quad (25a)$$

$$H_{\rho}^I = -(Y_0 k_z / k_0) E_{\phi}^I, \quad H_{\rho}^{II} = -(Y_2 k_z / k_2) E_{\phi}^{II} \quad (25b)$$

$$H_z^I = (Y_0 k_{\rho 1} / k_0) E_{\phi}^I, \quad H_z^{II} = (Y_2 k_{\rho 2} / k_2) E_{\phi}^{II} \quad (25c)$$

for  $TE^{in}$

where all other field components vanish and  $C_2$  and  $D_2$  are constants. Here superscript in indicates the interface mode. From the above results, we can see that the interface mode is well-approximated to the normal mode on the surface of a semi-infinite lossy material.

There exist two interface modes at most. The fields of the interface mode decay rapidly to both sides of the interface. The conditions for the interface mode to exist are easily recognized from Eqs. (24) and (25) to be

$$\text{Im}(k_{\rho 1} a) \gg 1 \quad (26)$$

and

$$-\text{Im}(k_{\rho 2} \tau) \gg 1 \quad (27a)$$

Using the boundary conditions at the interface, Eq. (27a) can be rewritten equivalently either

$$-\text{Im}(k_{\rho 1} \epsilon_2 \tau) \gg 1 \quad \text{for } TM^{in} \quad (27b)$$

or

$$-\text{Im}(k_{\rho 1} \mu_2 \tau) \gg 1 \quad \text{for } TE^{in} \quad (27c)$$

Thus for dielectric coating, only  $TM^{in}$  of the two modes can exist, and only the  $TE^{in}$  mode can be excited in a waveguide coated with a magnetic material.

#### IV. NUMERICAL RESULTS AND DISCUSSION

##### A. Lossless Coating

When the coating material is lossless, the normal modes in the overmoded coated waveguide become surface waves as the layer thickness increases, in the order of  $HE_{m1}$ ,  $EH_{m1}$ ,  $HE_{m2}$ ,  $EH_{m2}$ , ... ( $m \neq 0$ ) and  $EH_{01}$ ,  $HE_{01}$ ,  $EH_{02}$ ,  $HE_{02}$ , ... ( $m = 0$ ) [4]. These features of the normal modes are shown in Figure 10 (Figure 11) for a dielectric (magnetic) coating, where the radial wave numbers are plotted as a function of the layer thickness. The large imaginary part of a complex radial number indicates that the modal field shifts to the waveguide wall and the mode behaves as a surface mode. Note that the  $HE_{11}$  in the magnetic-coated guide becomes a surface mode with a much thinner coating layer than that in the dielectric-coated guide. Otherwise, the onset of a new surface mode occurs around every quarter-wavelength thickness as the layer thickness increases.

##### B. Slightly Lossy Coating

Figure 12 (Figure 13) shows the radial wave numbers of the normal modes in a circular guide coated with a slightly lossy dielectric (magnetic) material. The general trend of the normal mode with variation of the layer thickness remains similar to that for the waveguide coated with a lossless material (Figures 10 and 11). As shown in Figures 14 and 15, the mode with a large imaginary part of the complex radial number of a surface-wave type has a large attenuation constant. This is due to the fact that the surface mode has a large

field concentration within the lossy region near the waveguide wall. It is interesting to note that the  $HE_{11}$  in the magnetic-coated guide acquires a very large attenuation constant with a much thinner coating layer than that in the dielectric-coated guide. The higher-order modes also become surface modes and acquire large attenuation constants only at a much thicker coating layer.

### C. Very Lossy Coating

When the coating material becomes very lossy, those features of the normal modes in the waveguide coated with a lossless material disappear. In fact, the propagation constant of the normal mode is independent of the layer thickness if the lossy layer is thicker than the skin depth of the normal mode (Figures 16 and 17). There is a mode separation between highly attenuated and lowly attenuated low-order modes. The highly attenuated modes in a dielectric-coated guide are usually lowly attenuated modes in magnetic-coated guide and vice versa (Figures 18 and 19). In general, the mode separation is less distinctive for higher-order modes.

When  $a/\lambda$  is large and the coating material is lossy enough, most of the low-order modes are inner modes which are mainly confined in the air region and the attenuation constants are small. Marcatali and Schmeltzer [5] evaluated the attenuation constants using the perturbation theory under the assumption that  $a/\lambda$  is large and the fields within the lossy region are small (see Section III). Figure 20 shows the comparison of the exact solutions with the approximate solutions by Marcatali and Schmeltzer for the attenuation constants of the normal modes in a dielectric-coated guide. Here the coating thickness  $\tau$  is fixed while  $a/\lambda$  is varied. We note that the exact and approximate solutions are in better agreement at a larger value of  $a/\lambda$ . The high-order modes usually require a large value of  $a/\lambda$  for good agreement between the exact and approximate solutions (see Section IIIA). This result indicates that the low-order modes become



excluded from the lossy layer near the wall at a smaller value of  $a/\lambda$  than do the high-order modes.

Figure 21 shows the comparison of the exact and various approximate solutions for the attenuation constants of the normal modes in a magnetic-coated circular guide. Most of the low-order modes become inner modes at a large value of  $a/\lambda$  as in the case of the dielectric coating (Figure 20). However, certain modes are confined near the wall. The  $EH_{11}$  mode at a large  $a/\lambda$  becomes a surface mode (Section IIIB), whose fields are mainly confined within the lossy region and have a large attenuation constant. The exact solution of the attenuation constant is well-approximated by the solution for the surface mode given in Eq. (17). The existence of the surface mode in a waveguide coated with a lossy material depends on whether the characteristic equation (Eq. (16)) has a solution close to the value for a surface mode (Eq. (17) or (18)). Also note that the  $HE_{12}$  mode becomes an interface mode (Section IIIC) whose fields are limited to the region near the interface between the air and lossy material. The attenuation constant of the interface mode is well-approximated by that of the mode on the surface of a semi-infinite lossy material. The criteria for the existence of the interface modes in a coated guide are given in Eqs. (26) and (27). Thus the attenuation constant of the interface mode is not as large as that of the surface mode but much larger than that of the inner mode (Figure 21).

In Figures 20 and 21, the mode names in the parentheses for the inner modes correspond to the mode names by Marcatili and Schmeltzer [5], where the field diagrams of those modes are also shown. The surface mode does not exist when the lossy layer becomes infinitely extended. However, the interface mode should exist in a hollow lossy circular guide if the conditions in Eq. (26) and (27) are satisfied.

#### D. Mode Suppressor

So far, we have seen that the attenuation properties of the normal modes in a coated waveguide depend on the coating material, layer thickness and frequency. When the coating material is not very lossy, the attenuation constants of the normal modes strongly vary with the layer thickness. Since each mode has its own region where the mode is significantly attenuated, the coated guide can be used as a simple mode suppressor [12]. The device will be especially useful for eliminating low-order modes. Since low-order modes are mainly responsible for the radar cross section (RCS) at a small incident angle from a cavity-type structure, coating the cavity wall with a lossy material will be effective in reducing the RCS due to the undesirable interior irradiation from the normal modes in a cavity [13], [14]. In a practical design, the transition region between the uncoated and coated sections of the waveguide must be long enough to prevent any mode conversion [15].

#### E. CP Antenna

When the coating material is sufficiently lossy and  $a/\lambda$  is large, most of the normal modes become inner modes if the coating layer is thick enough, i.e., thicker than the skin depths of the modal fields. Both the magnetic and electric fields of the inner mode are small near the waveguide wall. The  $HE_{11}$  mode in the waveguide coated with a lossy magnetic material becomes an inner mode at a much smaller value of  $a/\lambda$  than that with a lossy dielectric material. The boundary conditions of the  $HE_{11}$  mode in this case are similar to those of a corrugated waveguide [16] - [19]; hence, this waveguide can be used as an alternate to the corrugated waveguide to produce circularly polarized radiation or reduce the side-lobe level. Even though the loss of the  $HE_{11}$  mode in the coated waveguide may be higher than that of a well-designed corrugated

waveguide, the coated waveguide is cheaper to build and lighter in weight than the corrugated waveguide, as explained in [20].

## V. CONCLUSION

The normal modes in a circular guide coated with a lossy material are classified and analyzed, emphasizing the attenuation properties of the normal modes. It is shown that the coating material should not be too lossy for the low-order modes to be significantly attenuated. A much thinner coating layer is required for the attenuation of the  $HE_{11}$  mode when the coating material is magnetic rather than dielectric. The coating technique is especially useful in reducing the radar cross section from a jet engine inlet, a subject that will be reported by us in a future communication.

When  $a/\lambda$  is large and the coating material is very lossy, most of the low-order modes become inner modes, which have small fields within the lossy region and small attenuation constants. An interesting application of the  $HE_{11}$  mode in an open-ended waveguide coated with a very lossy magnetic material is that it can be used for circularly polarized radiation [20].

## REFERENCES

- [1] M. Miyagi, A. Hongo, and S. Kawakami, "Transmission characteristics of dielectric-coated metallic waveguide for infrared transmission: slab waveguide model," IEEE J. Quantum Electron., vol. QE-19, pp. 136-145, February 1983.
- [2] H. G. Unger, "Lined waveguide," Bell System Tech. J., vol. 41, pp. 745-768, March 1962.
- [3] J. W. Carlin and P. D'Agostino, "Low-loss modes in dielectric lined waveguide," Bell System Tech. J., vol. 50, pp. 1631-1638, May-June 1971.
- [4] J. W. Carlin and P. D'Agostino, "Normal modes in overmoded dielectric-lined circular waveguide," Bell System Tech. J., vol. 52, pp. 453-486, April 1973.

- [5] E. A. J. Marcatili and R. A. Schmeltzer, "Hollow metallic and dielectric waveguides for long distance optical transmission and lasers," Bell System Tech. J., pp. 1783-1809, July 1964.
- [6] C. Dragone, "High-frequency behavior of waveguides with finite surface impedances," Bell System Tech. J., vol. 60, pp. 89-116, January 1981.
- [7] P. J. B. Clarricoats, "Propagation along unbounded and bounded dielectric rods," Part 1 and Part 2, Proc. IEE, Mon. 409E and 410E, pp. 170-186, October 1960.
- [8] G. N. Tsandoulas and W. J. Ince, "Modal inversion in circular waveguides-part 1: theory and phenomenology," IEEE Trans. Microwave Theory Tech., vol. MTT-19, pp. 386-392, April 1971.
- [9] G. N. Tsandoulas, "Bandwidth enhancement in dielectric-lined circular waveguides," IEEE Trans. Microwave Theory Tech., vol. MTT-21, pp. 651-654, October 1973.
- [10] C. S. Lee, S. L. Chuang, S. W. Lee, and Y. T. Lo, "Wave attenuation and mode dispersion in a waveguide coated with lossy dielectric material," Univ. of Illinois Electromagnetics Laboratory, Urbana, IL, Technical Report, No. 84-13, July 1984.
- [11] R. F. Harrington, Time Harmonic Electromagnetic Fields. New York: McGraw-Hill Book Co., 1961.
- [12] T. N. Anderson, "Low loss transmission using overmoded waveguide, a practical 1981 review of the state of the art," presented at the IEEE AP/MTT-S, Philadelphia Section, Benjamin Franklin 1981 Symposium on Advances in Antenna and Microwave Technology, May 1981.
- [13] S. W. Lee, Y. T. Lo, S. L. Chuang, and C. S. Lee, "Numerical methods for analyzing electromagnetic scattering," Semiannual Report to NASA Lewis Research Center, Cleveland, Ohio, March 1985.
- [14] H. R. Witt and E. L. Price, "Scattering from hollow conducting cylinders," Proc. IEE, vol. 115, pp. 94-99, January 1968.
- [15] H. Unger, "Circular waveguide taper of improved design," Bell System Tech. J., vol. 37, pp. 899-912, July 1958.
- [16] M. J. Al-Hakkak and Y. T. Lo, "Circular waveguide and horns with anisotropic and corrugated boundaries," Antenna Laboratory Report No. 73-3, University of Illinois, Urbana, Illinois, 1973.
- [17] P. J. B. Clarricoats, A. D. Olver, and S. L. Chong, "Attenuation in corrugated circular waveguide, Part 1, Theory," Proc. IEE, vol. 122, pp. 1173-1179, 1975.
- [18] C. Dragone, "Reflection and mode conversion in a corrugated feed," Bell System Tech. J., vol. 56, pp. 835-867, 1977.

- [19] C. Dragone, "Attenuation and radiation characteristics of the HE mode," IEEE Trans. Microwave Theory Tech., vol. MTT-28, pp. 704-710, 1980.
- [20] C. S. Lee, S. L. Chuang, and S. W. Lee, "A simple version of corrugated waveguide: smooth-walled circular waveguide coated with lossy magnetic material," AP-S International Symposium Digest, vol. 1, pp. 303-306, 1985.
- [21] M. Abramowitz and I. A. Stegun, Handbook of Mathematical Functions. New York: Dover, 1972.

#### APPENDIX 1.

##### DEGENERACY BETWEEN THE CUTOFF FREQUENCIES OF THE $TM_{11}$ AND $TE_{01}$ MODES IN A DIELECTRIC-COATED CIRCULAR WAVEGUIDE

At the cutoff frequency ( $k_z = 0$ ), the characteristic equation in Eq. (1) becomes

$$\begin{aligned}
 & J_1'(k_{CM}a) [J_1(k_{CM2}a) N_1(k_{CM2}b) - N_1(k_{CM2}a) J_1(k_{CM2}b)] \\
 & - \sqrt{\epsilon_2/\mu_2} J_1(k_{CM}a) [J_1(k_{CM2}a) N_1(k_{CM2}b) - N_1'(k_{CM2}a) J_1(k_{CM2}b)] = 0
 \end{aligned}$$

for  $TM_{11}$  (A1.1)

or

$$\begin{aligned}
 & J_0'(k_{CE}a) [J_0(k_{CE2}a) N_0(k_{CE2}b) - N_0(k_{CE2}a) J_0'(k_{CE2}b)] \\
 & - \sqrt{\mu_2/\epsilon_2} J_0(k_{CE}a) [J_0'(k_{CE2}a) N_0(k_{CE2}b) - N_0'(k_{CE2}a) J_0(k_{CE2}b)] = 0
 \end{aligned}$$

for  $TE_{01}$  (A1.2)

where

$$k_{CM} = \frac{2\pi}{c} f_{CM} \quad , \quad k_{CM2} = k_{CM} \sqrt{\epsilon_2 \mu_2}$$

$$k_{CE} = \frac{2\pi}{c} f_{CE} \quad , \quad k_{CE2} = k_{CE} \sqrt{\epsilon_2 \mu_2}$$

Here  $f_{CM}$  and  $f_{CE}$  are the cutoff frequencies for the  $TM_{11}$  and  $TE_{01}$  modes, respectively.

Using the recurrence relations of Bessel functions [21], the derivative expressions in Eqs. (A1.1) and (A1.2) can be eliminated, and we obtain

$$\begin{aligned}
 & J_1(k_{CM}a) [J_0(k_{CM2}a) N_1(k_{CM2}b) - N_0(k_{CM2}a) J_1(k_{CM2}b)] \\
 & - [\sqrt{\mu_2/\epsilon_2} J_0(k_{CM}a) - (1/\sqrt{\epsilon_2\mu_2} - \sqrt{\mu_2/\epsilon_2})/k_{CM}a] [J_1(k_{CM2}a) N_1(k_{CM2}b) \\
 & - N_1(k_{CM2}a) J_1(k_{CM2}b)] = 0 \quad (A1.3)
 \end{aligned}$$

for  $TM_{11}$

and

$$\begin{aligned}
 & J_1(k_{CE}a) [J_0(k_{CE2}a) N_1(k_{CE2}b) - N_0(k_{CE2}a) J_1(k_{CE2}b) \\
 & - \sqrt{\mu_2/\epsilon_2} J_0(k_{CE}a) [J_1(k_{CE2}a) N_1(k_{CE2}b) - N_1(k_{CE2}a) J_1(k_{CE2}b)] = 0
 \end{aligned}$$

for  $TE_{01}$  (A1.4)

When  $\mu_2 = 1$ , the two characteristic equations are identical, and the cutoff frequencies of the  $TM_{11}$  and  $TE_{01}$  modes are the same. On the other hand, when the coating material is magnetic ( $\mu_2 \neq 1$ ), the degeneracy of these two modes at their cutoff frequencies is not present.

## APPENDIX 2

### FIELDS OF THE NORMAL MODES IN A COATED CIRCULAR GUIDE WHEN $k_{\rho 1} = 0$ (DIRECT METHOD).

From Maxwell's equations, we obtain four equations for the normal modes in a circular guide,

$$\nabla \times \nabla \times \vec{E} - k_0^2 \vec{E} = 0 \quad (\text{A2.1a})$$

$$\nabla \cdot \vec{E} = 0 \quad (\text{A2.1b})$$

First consider the case for  $m \neq 0$ . Due to the symmetry of the problem, we can assume that

$$E_\rho = R_\rho(\rho) \cos m\phi e^{-jk_z z} \quad (\text{A2.2a})$$

$$E_\phi = R_\phi(\rho) \sin m\phi e^{-jk_z z} \quad (\text{A2.2b})$$

$$E_z = R_z(\rho) \cos m\phi e^{-jk_z z} \quad (\text{A2.2c})$$

Since  $k_{\rho 1} = 0$ , from the dispersion relation

$$k_z = k_0 \quad (\text{A2.3})$$

Substituting Eq. (A2.2) in Eq. (A2.1), three linearly independent equations are obtained:

$$\rho \frac{d}{d\rho} \left[ \rho \left( \frac{dR_\rho(\rho)}{d\rho} \right) \right] - m^2 R_\rho(\rho) = 0 \quad (\text{A2.4a})$$

$$m\rho \frac{d}{d\rho} [\rho R_\phi(\rho)] + m^2 R_\rho(\rho) - jk_0 \rho^2 \frac{dR_z(\rho)}{d\rho} = 0 \quad (\text{A2.4b})$$

$$\frac{d}{d\rho} [\rho R_\rho(\rho)] + m R_\phi(\rho) - jk_0 \rho R_z(z) = 0 \quad (\text{A2.4c})$$

Solving these coupled equations, the fields in Region I ( $m \neq 0$ ) are given by

$$E_{\rho}^I = (C_1 \rho^{m+1} + C_2 \rho^{m-1}) \cos m\phi \quad (\text{A2.5a})$$

$$E_{\phi}^I = (C_1 \rho^{m+1} - C_2 \rho^{m-1}) \sin m\phi \quad (\text{A2.5b})$$

$$E_z^I = \frac{2(m+1) C_1}{jk_0} \rho^m \cos m\phi \quad (\text{A2.5c})$$

$$H_{\rho}^I = -Y_0 \left[ C_1 \rho^{m+1} + \left( \frac{2m(m+1) C_1}{k_0^2} - C_2 \right) \rho^{m-1} \right] \sin m\phi \quad (\text{A2.5d})$$

$$H_{\phi}^I = Y_0 \left[ C_1 \rho^{m+1} - \left( \frac{2m(m+1) C_1}{k_0^2} - C_2 \right) \rho^{m-1} \right] \cos m\phi \quad (\text{A2.5e})$$

$$H_z^I = -Y_0 \frac{2(m+1) C_1}{jk_0} \rho^m \sin m\phi \quad (\text{A2.5f})$$

Using Eq. (A2.3), the fields in Region II ( $m \neq 0$ ) are obtained from Eq. (2):

$$E_{\rho}^{II} = - \left[ \frac{D_1}{\sqrt{\epsilon_2 \mu_2}} G_3'(\rho) + \frac{D_2^m}{k_{\rho 2} \rho} G_4(\rho) \right] \cos m\phi \quad (\text{A2.6a})$$

$$E_{\phi}^{II} = \left[ \frac{D_1^m}{\sqrt{\epsilon_2 \mu_2} k_{\rho 2} \rho} G_3(\rho) + D_2 G_4'(\rho) \right] \sin m\phi \quad (\text{A2.6b})$$

$$E_z^{II} = \frac{D_1 k_{\rho 2}}{jk_2} G_3(\rho) \cos m\phi \quad (\text{A2.6c})$$

$$H_{\rho}^{II} = -Y_2 \left[ \frac{D_1^m}{k_{\rho 2} \rho} G_3(\rho) + \frac{D_2}{\sqrt{\epsilon_2 \mu_2}} G_4'(\rho) \right] \sin m\phi \quad (\text{A2.6d})$$

$$H_{\phi}^{II} = - \left[ Y_2 D_1 G_3'(\rho) + \frac{D_2^m}{\sqrt{\epsilon_2 \mu_2} k_{\rho 2} \rho} G_4(\rho) \right] \cos m\phi \quad (\text{A2.6e})$$



$$H_z^{II} = Y_2 \frac{D_2 k_{\rho 2}}{j k_2} G_4(\rho) \sin m\phi \quad (A2.6f)$$

where

$$G_3(\rho) = J_m(k_{\rho 2}\rho) N_m(k_{\rho 2}b) - N_m(k_{\rho 2}\rho) J_m(k_{\rho 2}b) \quad (A2.6g)$$

$$G_3'(\rho) = J_m'(k_{\rho 2}\rho) N_m(k_{\rho 2}b) - N_m'(k_{\rho 2}\rho) J_m(k_{\rho 2}b) \quad (A2.6h)$$

$$G_4(\rho) = J_m(k_{\rho 2}\rho) N_m'(k_{\rho 2}b) - N_m(k_{\rho 2}\rho) J_m'(k_{\rho 2}b) \quad (A2.6i)$$

$$G_4'(\rho) = J_m'(k_{\rho 2}\rho) N_m'(k_{\rho 2}b) - N_m'(k_{\rho 2}\rho) J_m'(k_{\rho 2}b) \quad (A2.6j)$$

Note that the convention of  $e^{j(\omega t - k_0 z)}$  is understood and omitted. Here

$k_{\rho 2} = \sqrt{\epsilon_2 \mu_2 - 1} k_0$ , and  $C_1$ ,  $G_2$ ,  $D_1$  and  $D_2$  are constants to be determined by imposing the boundary conditions at the interface between the air and material regions. These constants are related by

$$C_1 = \frac{G_3(a) k_{\rho 2} D_1}{\sqrt{\epsilon_2 \mu_2} 2(m+1) a^m} \quad (A2.7a)$$

$$D_2 = -\sqrt{\mu_2/\epsilon_2} \frac{G_3(a)}{G_4(a)} D_1 \quad (A2.7b)$$

$$C_2 = a^2 C_1 - \left[ \frac{D_1 m G_3(a)}{\sqrt{\epsilon_2 \mu_2} k_{\rho 2} a} + D_2 G_4'(a) \right] / a^{m-1} \quad (A2.7c)$$

The coating thickness is determined by the characteristic equation,

$$\frac{(k_{\rho 2} a)^2}{m+1} + (k_{\rho 2} a) \left[ \frac{G_3'(a)}{G_3(a)} \epsilon_2 + \frac{G_4'(a)}{G_4(a)} \mu_2 \right] - m(\epsilon_2 \mu_2 + 1) = 0 \quad (A2.8)$$

Note that the fields are neither TE nor TM and the fields in Region I do not show a Bessel-function dependence of radial distance.

The fields for  $m = 0$  can be similarly shown to be

$$E_{\rho}^I = \frac{jk_0 C_{10}}{2} \rho, \quad E_{\rho}^{II} = -\frac{j C_{20}}{\sqrt{\epsilon_2 \mu_2} - 1} G'_{30}(\rho) \quad (A2.9a)$$

$$H_{\phi}^I = Y_0 E_{\rho}^I, \quad H_{\phi}^{II} = Y_0 \epsilon_2 E_{\rho}^{II} \quad (A2.9b)$$

$$E_z^I = C_{10}, \quad E_z^{II} = C_{20} G_{30}(\rho) \quad \text{for TM}_{0n} \quad (A2.9c)$$

and

$$H_{\rho}^I = \frac{jk_0 D_{10}}{2} \rho, \quad H_{\rho}^{II} = -\frac{j D_{20}}{\sqrt{\epsilon_2 \mu_2} - 1} G'_{40}(\rho) \quad (A2.10a)$$

$$E_{\phi}^I = -H_{\rho}^I / Y_0, \quad E_{\phi}^{II} = -\mu_2 H_{\rho}^{II} / Y_0 \quad (A2.10b)$$

$$H_z^I = D_{10}, \quad H_z^{II} = D_{20} G_{40}(\rho) \quad \text{for TE}_{0n} \quad (A2.10c)$$

where  $G_{30}(\rho)$ ,  $G'_{30}(\rho)$ ,  $G_{40}(\rho)$  and  $G'_{40}(\rho)$  are  $G_3(\rho)$ ,  $G'_3(\rho)$ ,  $G_4(\rho)$  and  $G'_4(\rho)$  with  $m = 0$ , respectively. All other field components vanish, and  $C_{10}$ ,  $C_{20}$ ,  $D_{10}$  and  $D_{20}$  are constants which are related by

$$C_{10} = C_{20} G_{30}(a) \quad (A2.11a)$$

$$D_{10} = D_{20} G_{40}(a) \quad (A2.11b)$$

The coating thickness for  $m = 0$  is determined by the following characteristic equation,

$$G_{30}(a) + \frac{2\epsilon_2}{k_0 a \sqrt{\epsilon_2 \mu_2} - 1} G'_{30}(a) = 0 \quad \text{for TM}_{0n} \quad (A2.12a)$$

or

$$G_{40}(a) + \frac{2\mu_2}{k_0 a \sqrt{\epsilon_2 \mu_2 - 1}} G'_{40}(a) = 0 \quad \text{for TE}_{0n} \quad (\text{A2.12b})$$

The fields are either TE or TM and the fields in the air region show a linear dependence of radial distance instead of the usual Bessel-function dependence in the case of an uncoated guide.

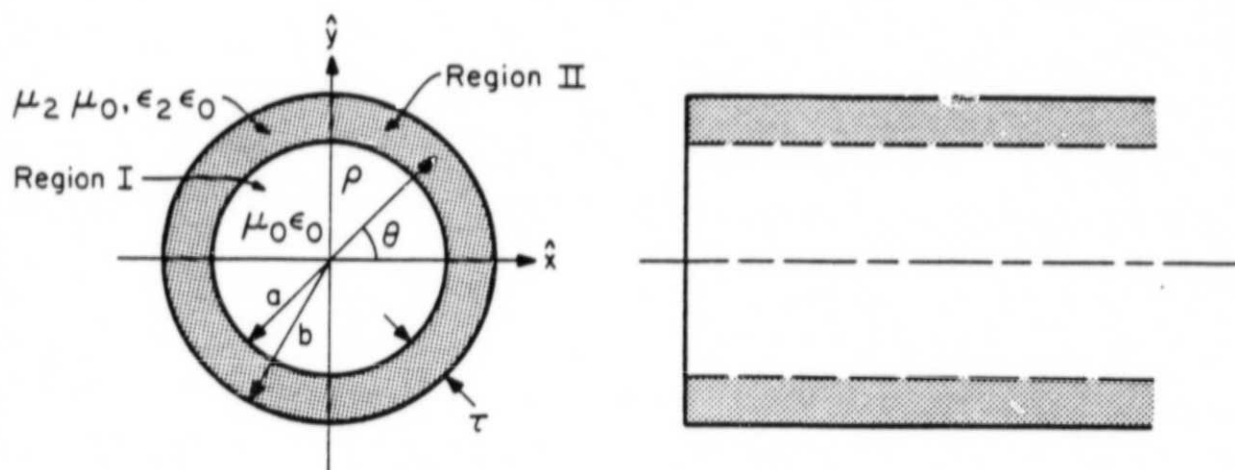


Figure 1. A coated circular waveguide.

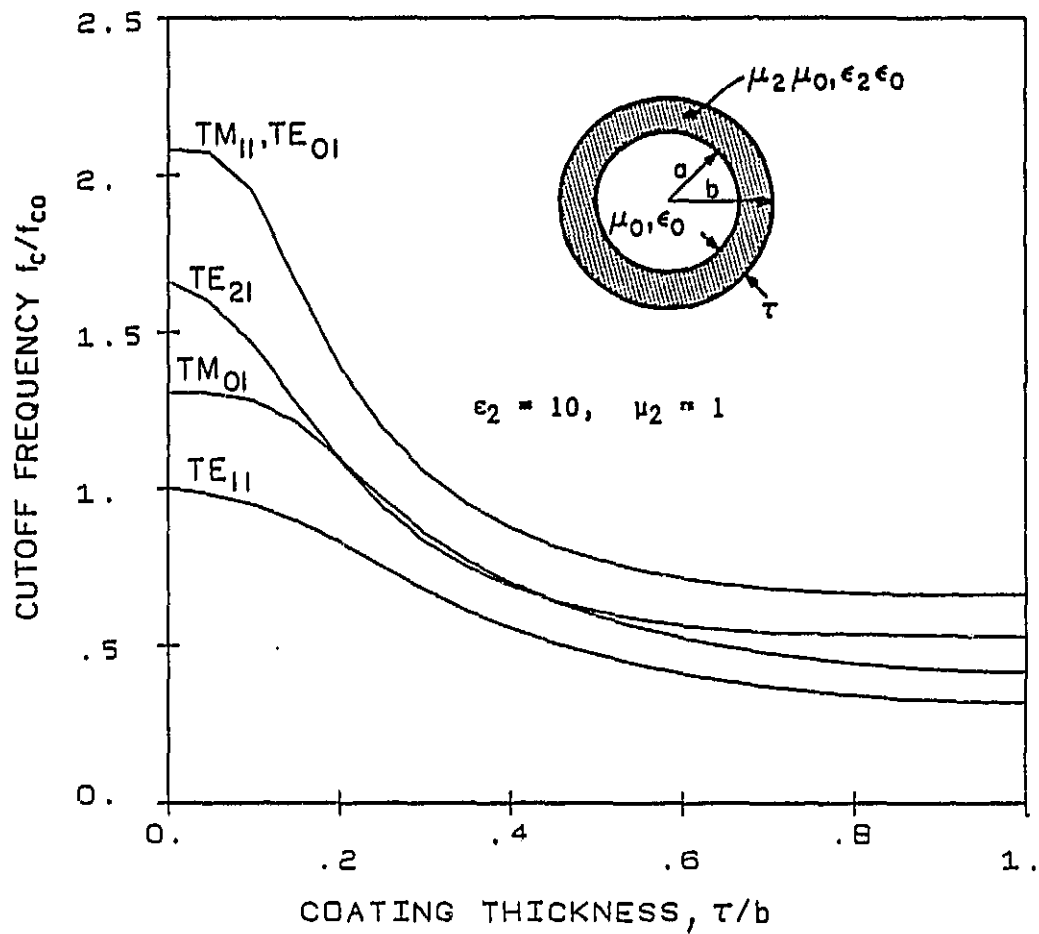


Figure 2. The cutoff frequencies in a dielectric-coated waveguide ( $\epsilon_2 = 10$ ,  $\mu_2 = 1$ ) normalized to that of the  $TE_{11}$  mode in an empty guide ( $f_{co}$ ) as a function of coating thickness.

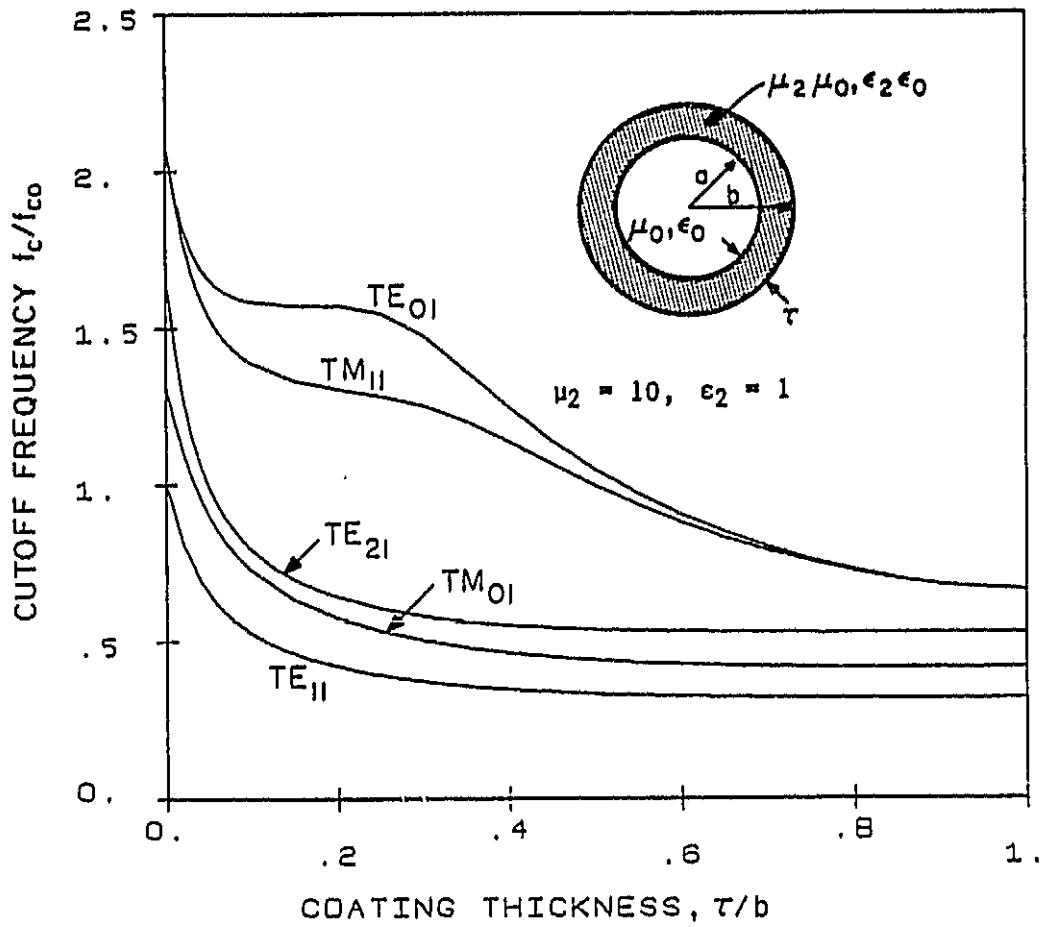


Figure 3. The cutoff frequencies in a magnetic-coated waveguide ( $\mu_2 = 10$ ,  $\epsilon_2 = 1$ ) normalized to that of the TE<sub>11</sub> mode in an empty guide ( $f_{co}$ ) as a function of coating thickness.

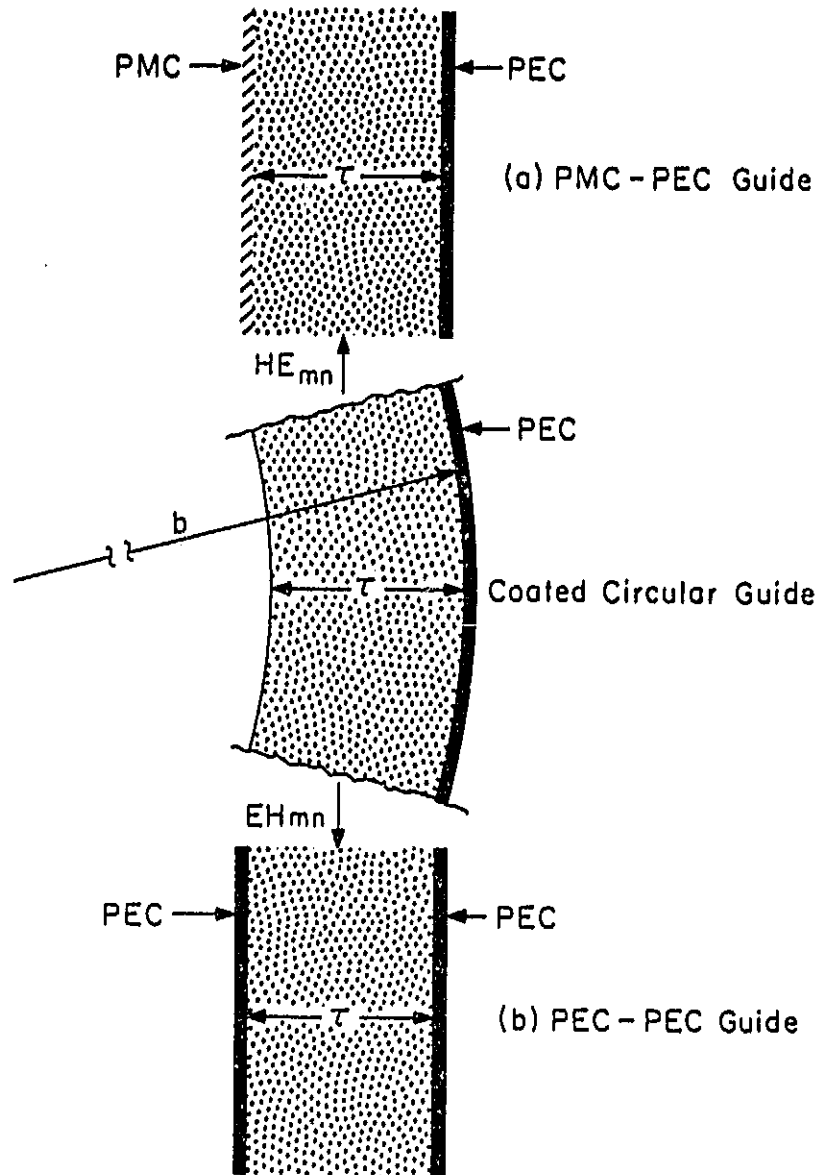


Figure 4. Mode transition in a coated circular guide at the high-frequency limit. The  $HE_{mn}$  modes approach modes in a PMC-PEC guide, and the  $EH_{mn}$  approach modes in PEC-PEC guide.

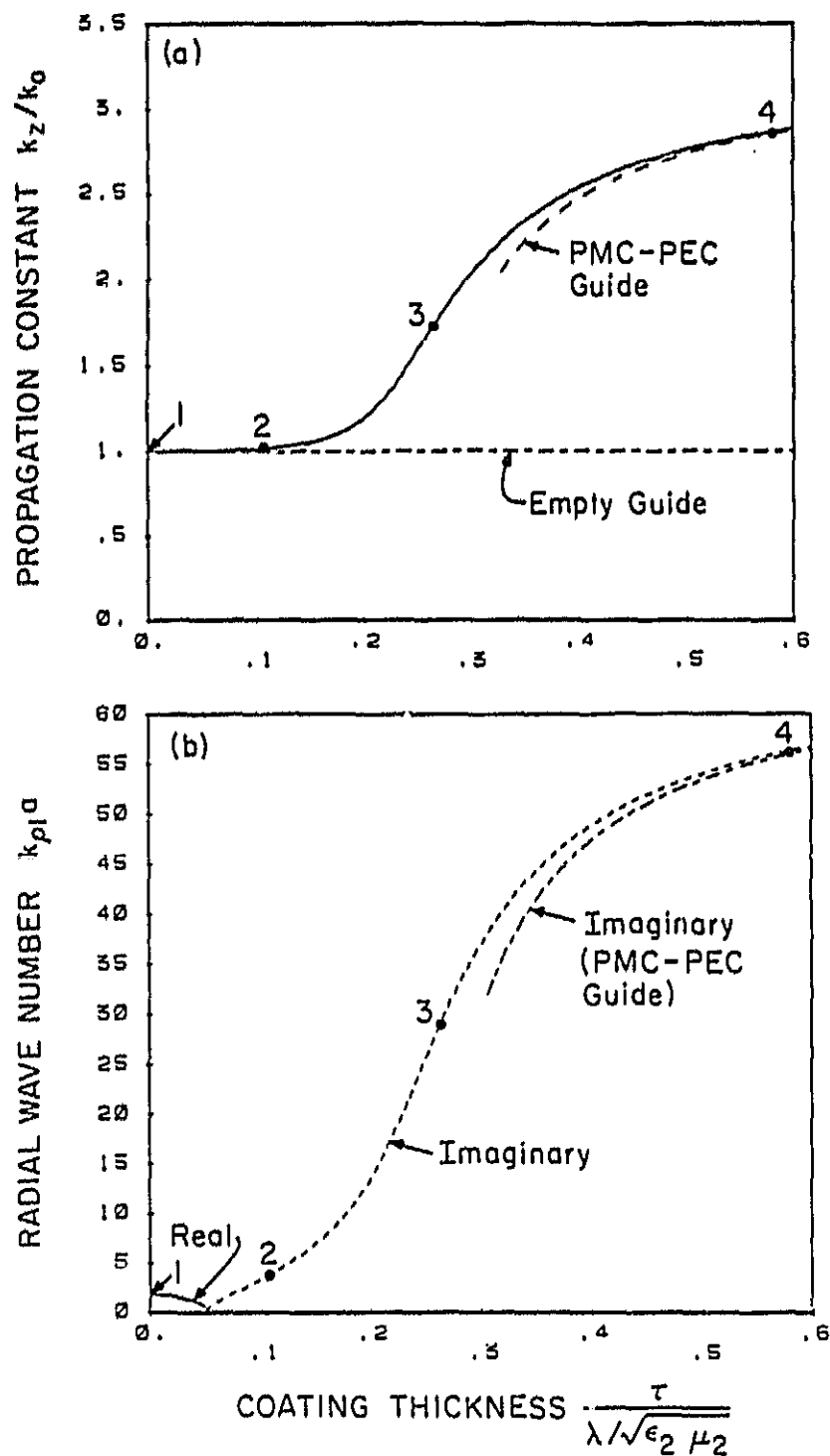


Figure 5. a) Normalized propagation constant and b) radial wave number ( $k_\rho a$ ) of the  $HE_{11}$  mode in a dielectric-coated waveguide ( $\epsilon_2 = 10, \mu_2 = 1$ ) as a function of the coating thickness in "effective" wavelength ( $\tau' = \tau\sqrt{\epsilon_2 \mu_2}/\lambda$ ). The power distributions for the four marked points are shown in Figure 6. The approximate solution of the surface mode using the two-slab model is also shown (see Section III).



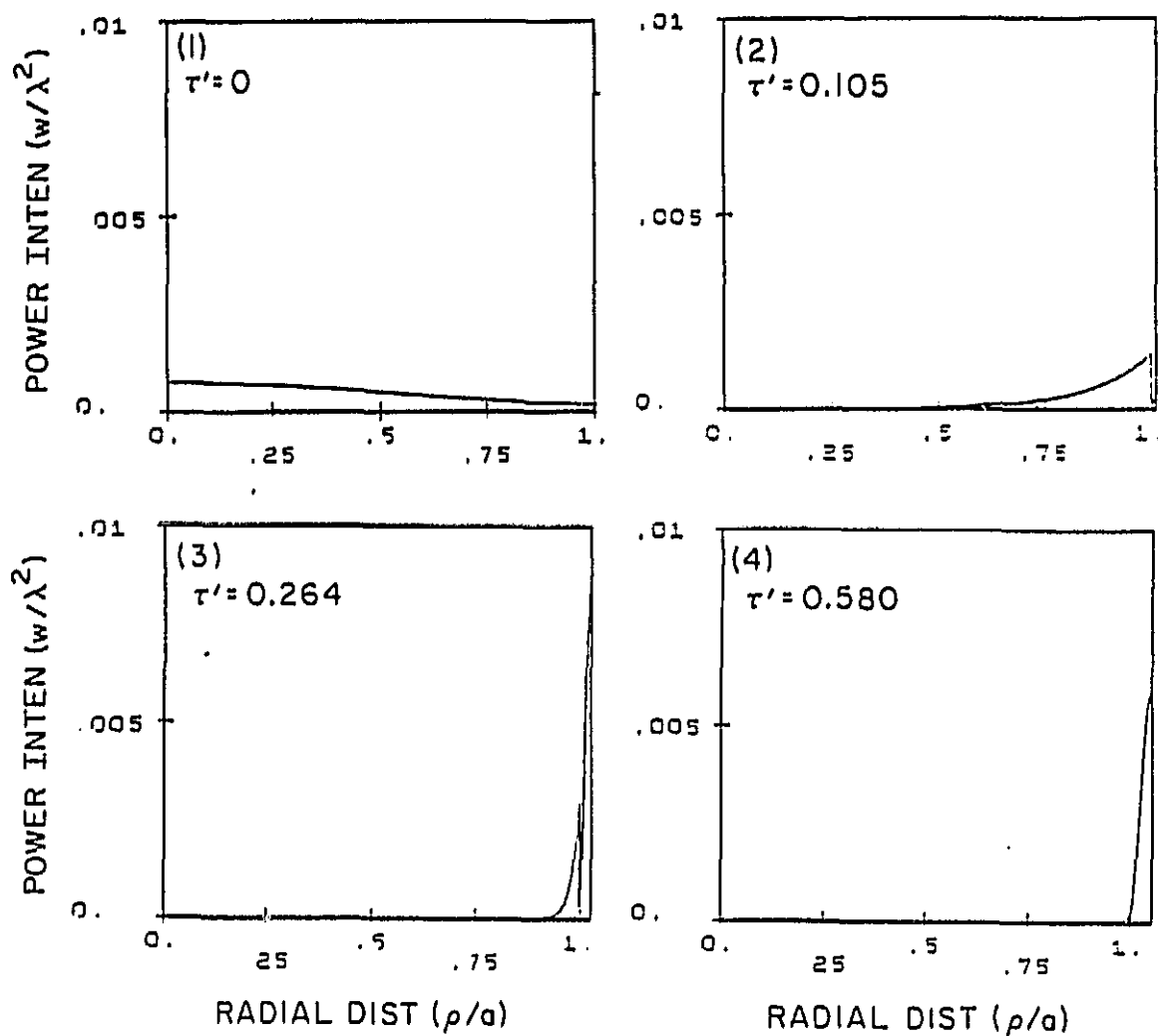


Figure 6. Normalized angle-averaged power distribution in watts/λ² as a function of radial distance in a dielectric-coated waveguide ( $\epsilon_2 = 10$ ,  $\mu_2 = 1$ ) with four different coating thicknesses. The corresponding points for these diagrams are marked in Figure 5 ( $\tau' = \tau\sqrt{\epsilon_2\mu_2}/\lambda$ ).

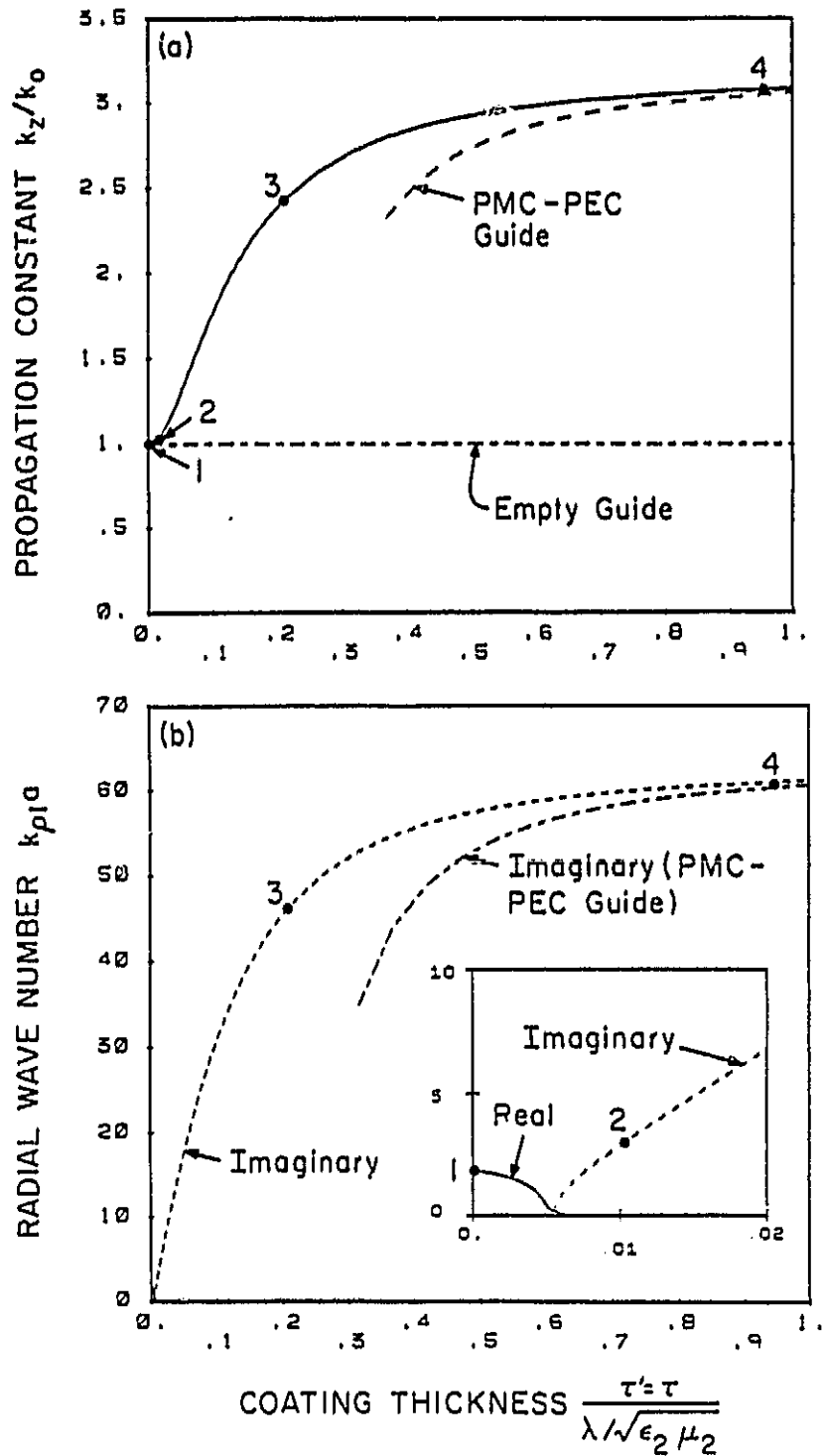


Figure 7. a) Normalized propagation constant and b) radial wave number ( $k_{\rho 1}a$ ) of the  $HE_{11}$  mode in a magnetic-coated waveguide ( $\mu_2 = 10, \epsilon_2 = 1$ ) as a function of the lining thickness in "effective" wavelength ( $\tau' = \tau \sqrt{\epsilon_2 \mu_2} / \lambda$ ). The power distributions of the four marked points are shown in Figure 8. The approximate solution of the surface mode using the two-slab model is also shown (see Section III).

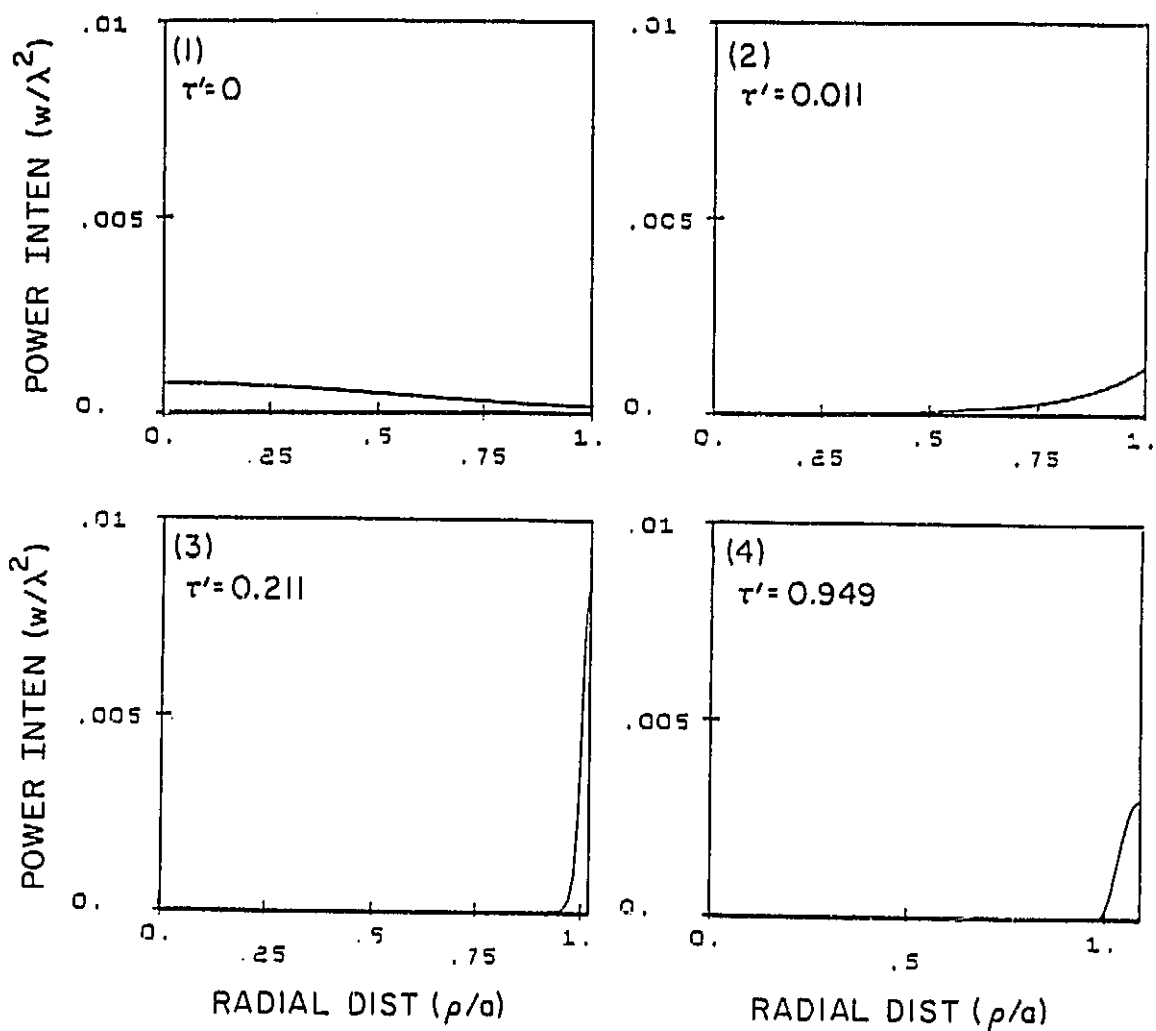


Figure 8. Normalized angle-averaged power distribution in watts/ $\lambda^2$  as a function of radial distance in a magnetic-coated waveguide ( $\mu_2 = 10$ ,  $\epsilon_2 = 1$ ) with four different coating thicknesses. The corresponding points for these diagrams are marked in Figure 7 ( $\tau' = \tau\sqrt{\epsilon_2\mu_2}/\lambda$ ).

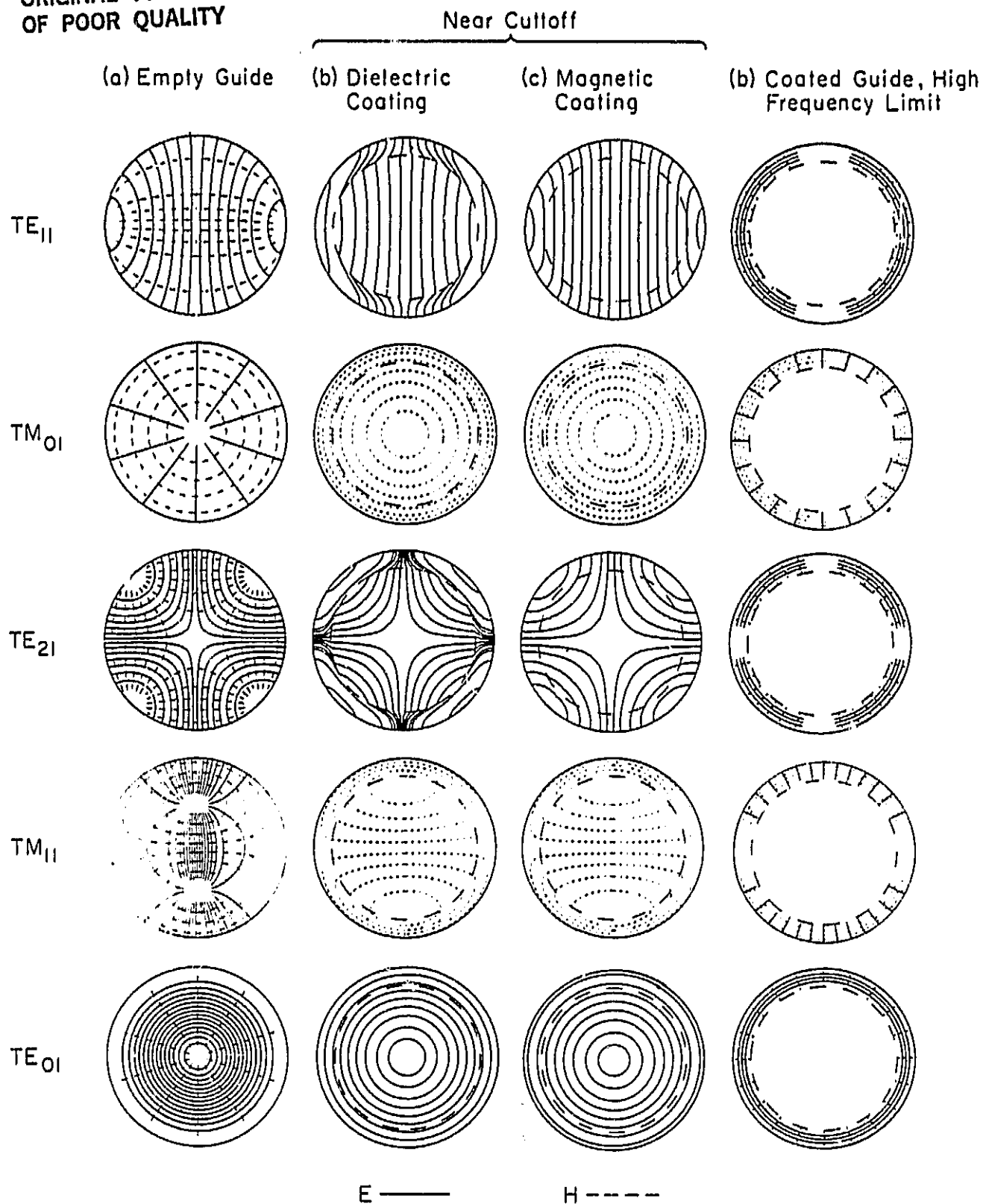


Figure 9. Transverse field distributions of the normal modes in a) empty guide, b) dielectric-coated guide at cutoff frequencies, c) magnetic-coated guide at cutoff frequencies and d) coated guide at the high-frequency limit.

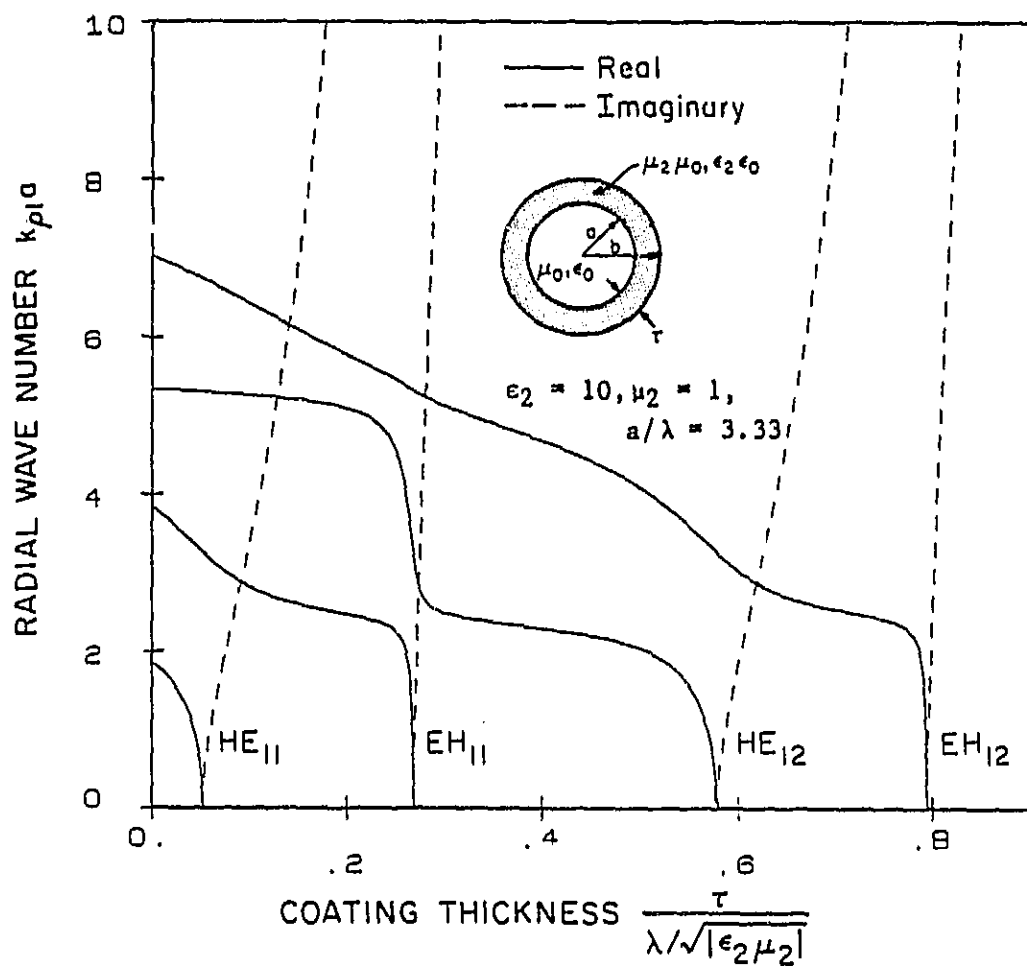


Figure 10. Radial wave numbers of the normal modes in a waveguide coated with lossless dielectric material ( $\epsilon_2 = 10, \mu_2 = 1, a/\lambda = 3.33$ ).

ORIGINAL PAGE IS  
OF POOR QUALITY

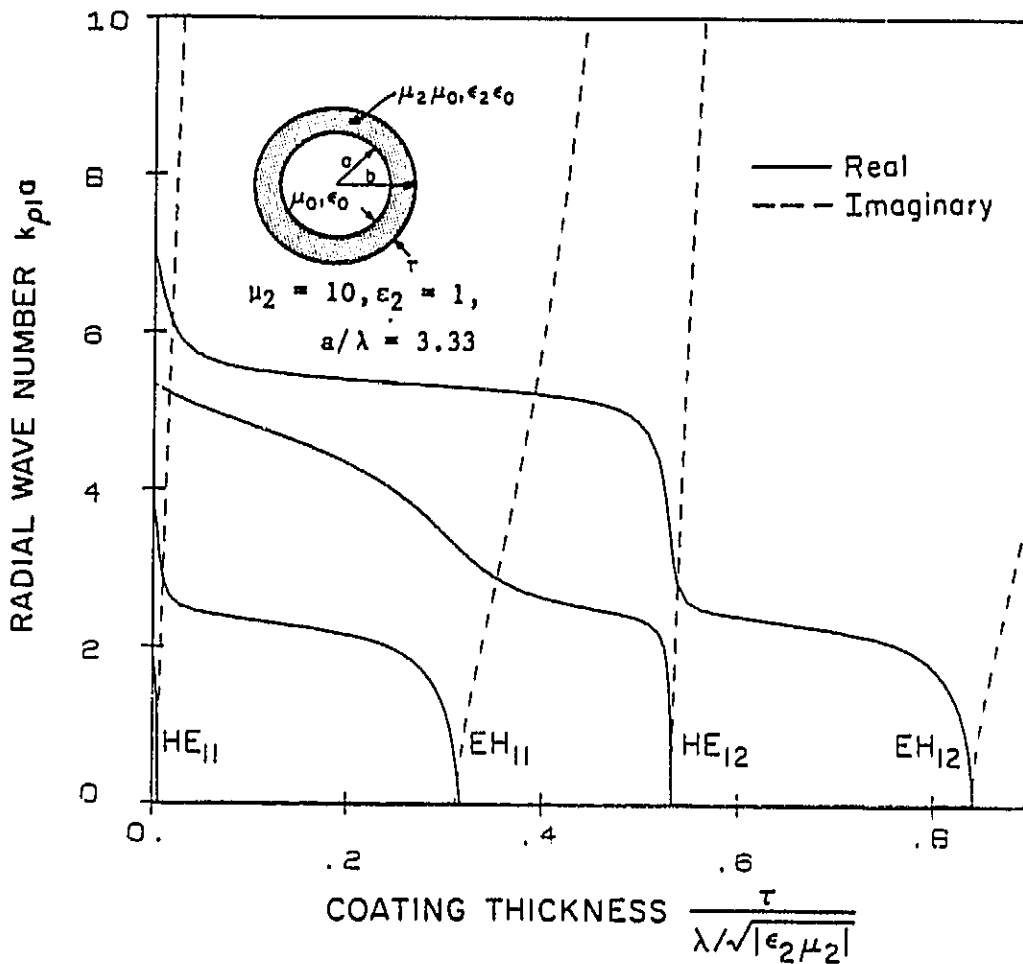


Figure 11. Radial wave numbers of the normal modes in a waveguide coated with a lossless magnetic material ( $\mu_2 = 10, \epsilon_2 = 1, a/\lambda = 3.33$ ).

ORIGINAL PAGE IS  
OF POOR QUALITY

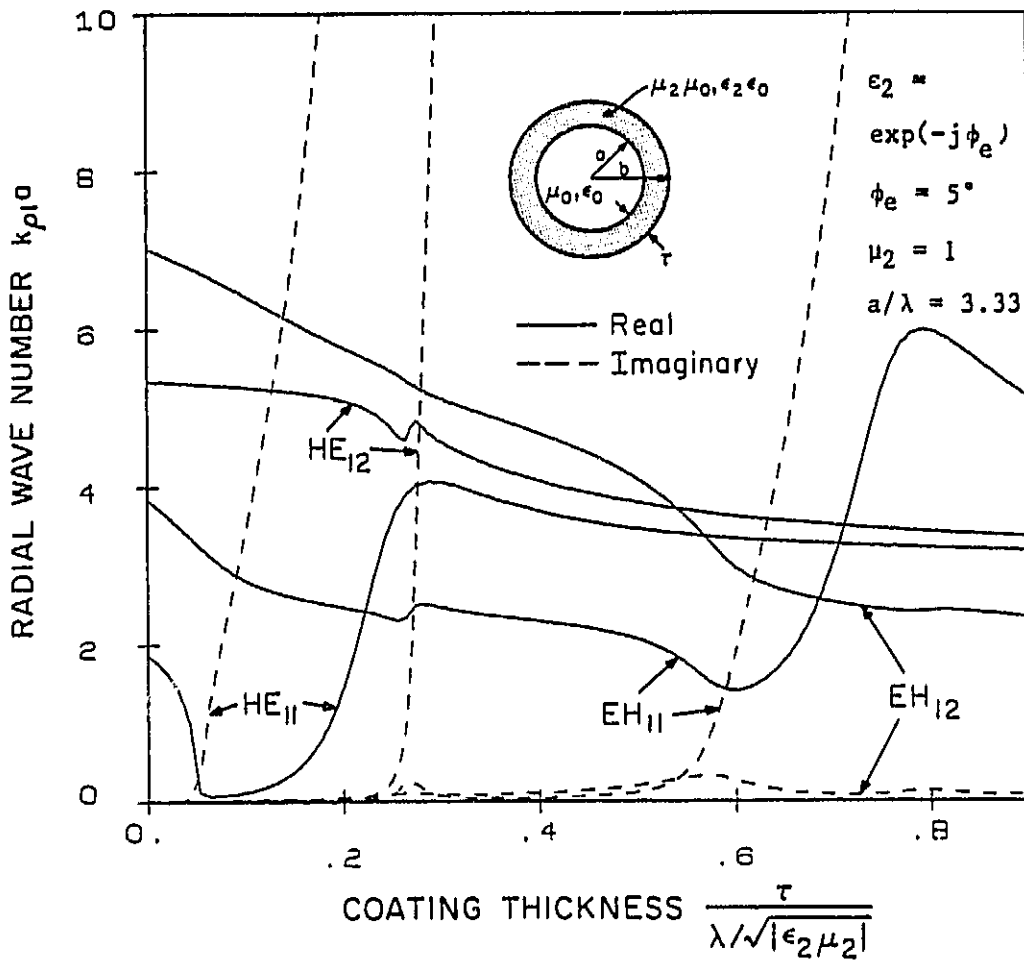


Figure 12. Radial wave numbers of the normal modes in a circular waveguide coated with a lossy dielectric material ( $\epsilon_2 = \exp(-j\phi_e)$ ,  $\phi_e = 5^\circ$ ,  $\mu_2 = 1$ ,  $a/\lambda = 3.33$ ).

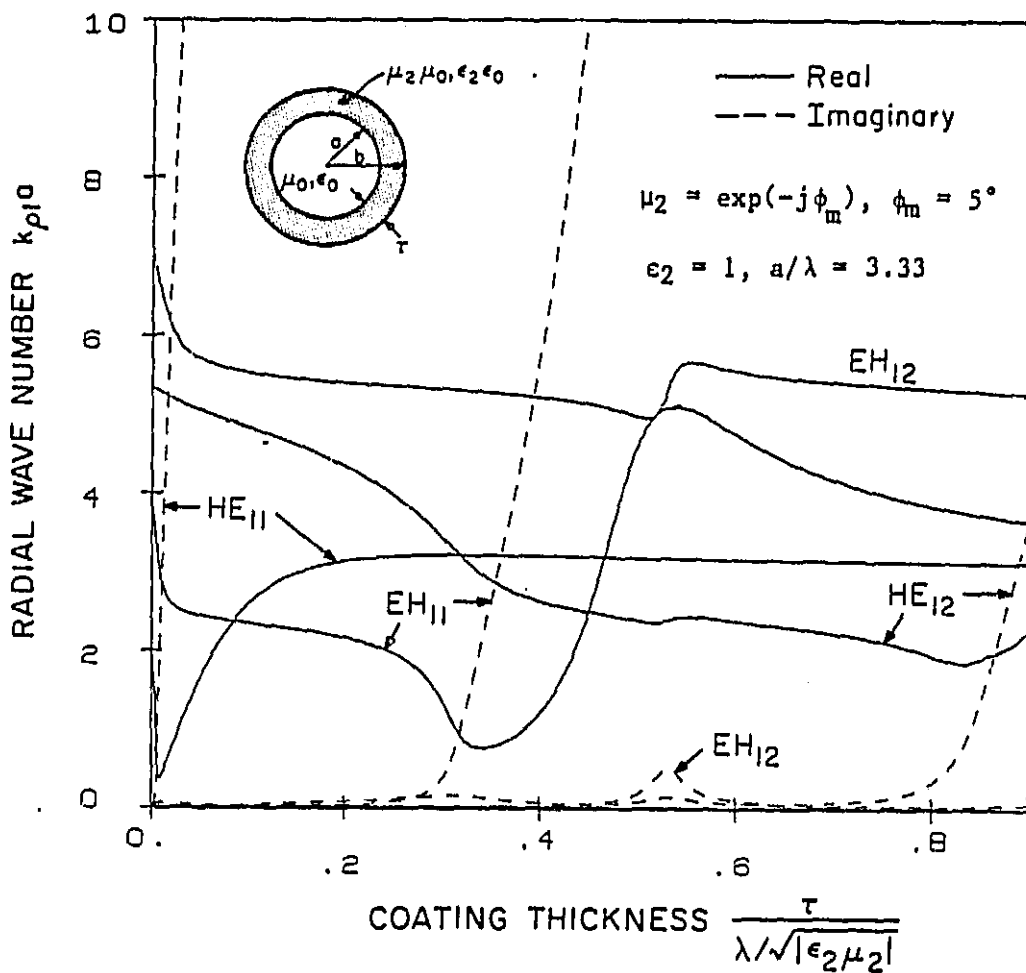


Figure 13. Radial wave numbers of the normal modes in a circular waveguide coated with a lossy magnetic material ( $\mu_2 = \exp(-j\phi_m)$ ,  $\phi_m = 5^\circ$ ,  $\epsilon_2 = 1$ ,  $a/\lambda = 3.33$ ).



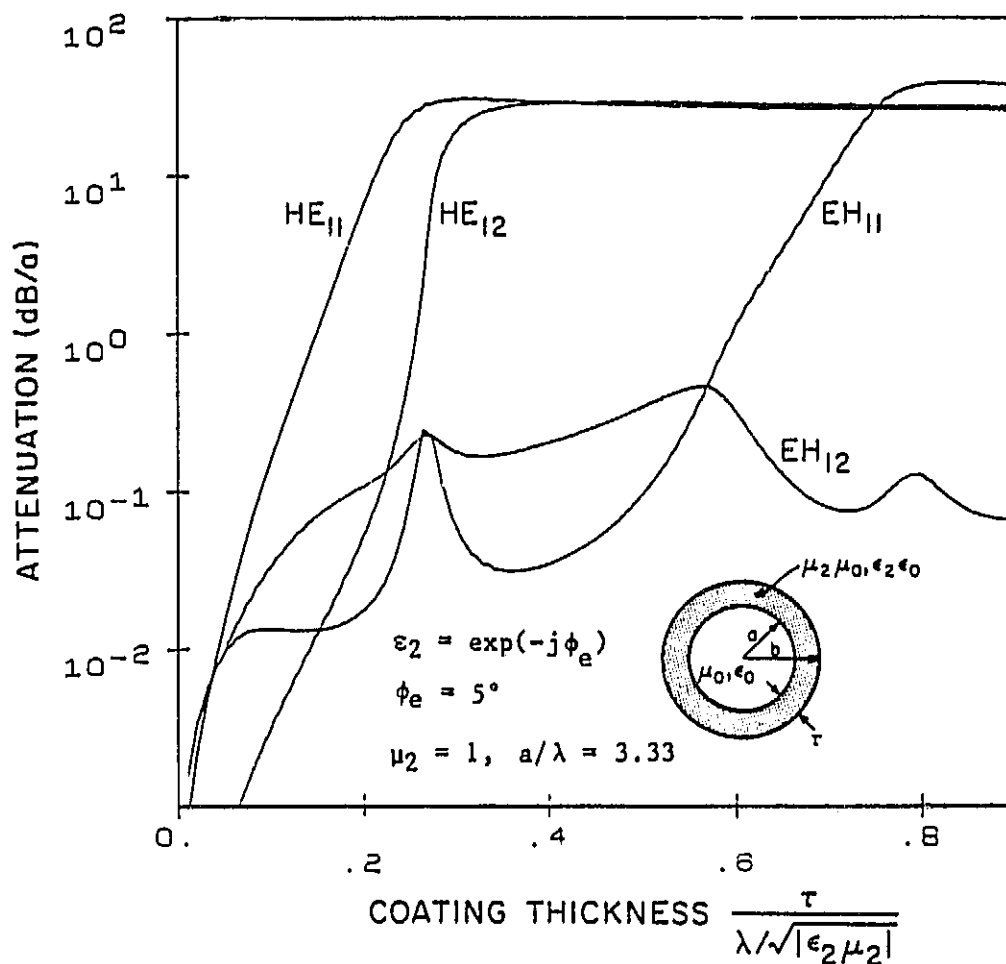


Figure 14. Attenuation constants of the normal modes in a circular waveguide coated with a lossy dielectric material ( $\epsilon_2 = \exp(-j\phi_e)$ ,  $\phi_e = 5^\circ$ ,  $\mu_2 = 1$ ,  $a/\lambda = 3.33$ ).

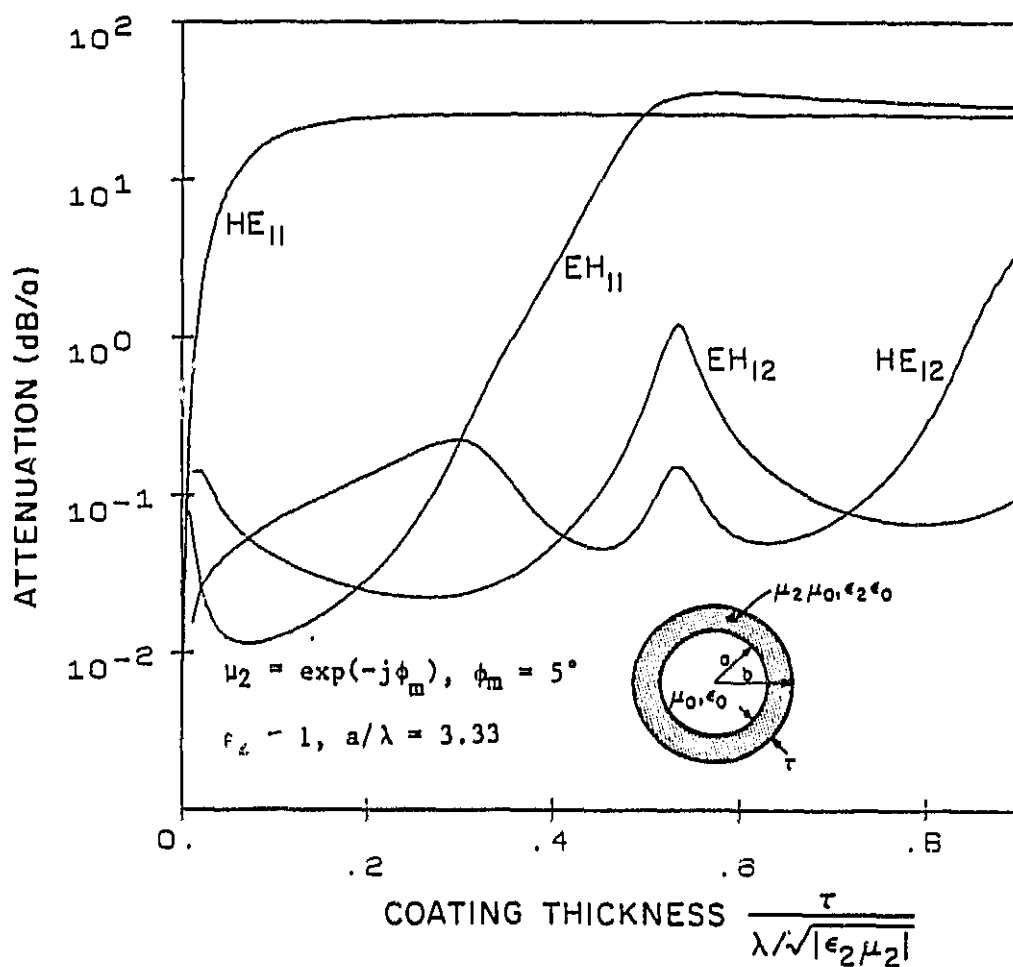


Figure 15. Attenuation constants of the normal modes in a circular waveguide coated with a lossy magnetic material ( $\mu_2 = \exp(-j\phi_m)$ ,  $\phi_m = 5^\circ$ ,  $\epsilon_2 = 1$ ,  $a/\lambda = 3.33$ ).

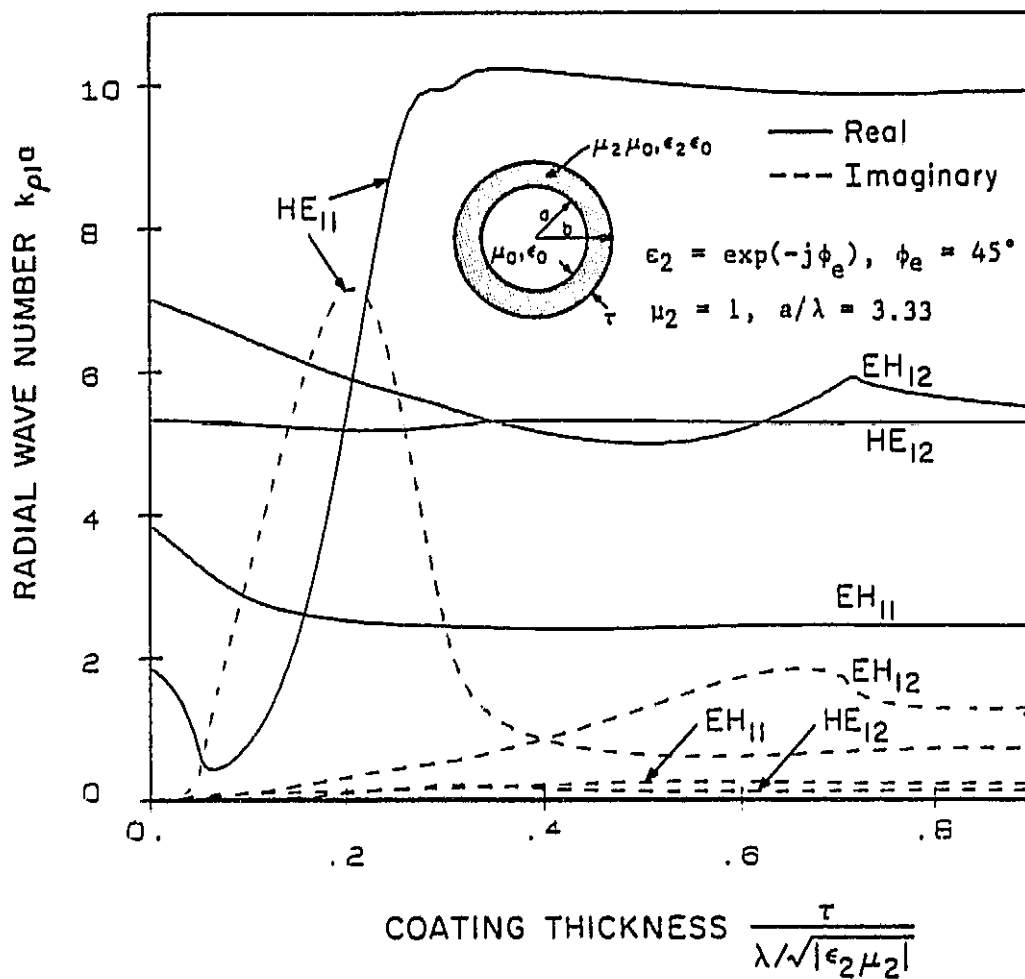


Figure 16. Radial wave numbers of the normal modes in a circular waveguide coated with a lossy dielectric material ( $\epsilon_2 = \exp(-j\phi_e)$ ,  $\phi_e = 45^\circ$ ,  $\mu_2 = 1$ ,  $a/\lambda = 3.33$ ).

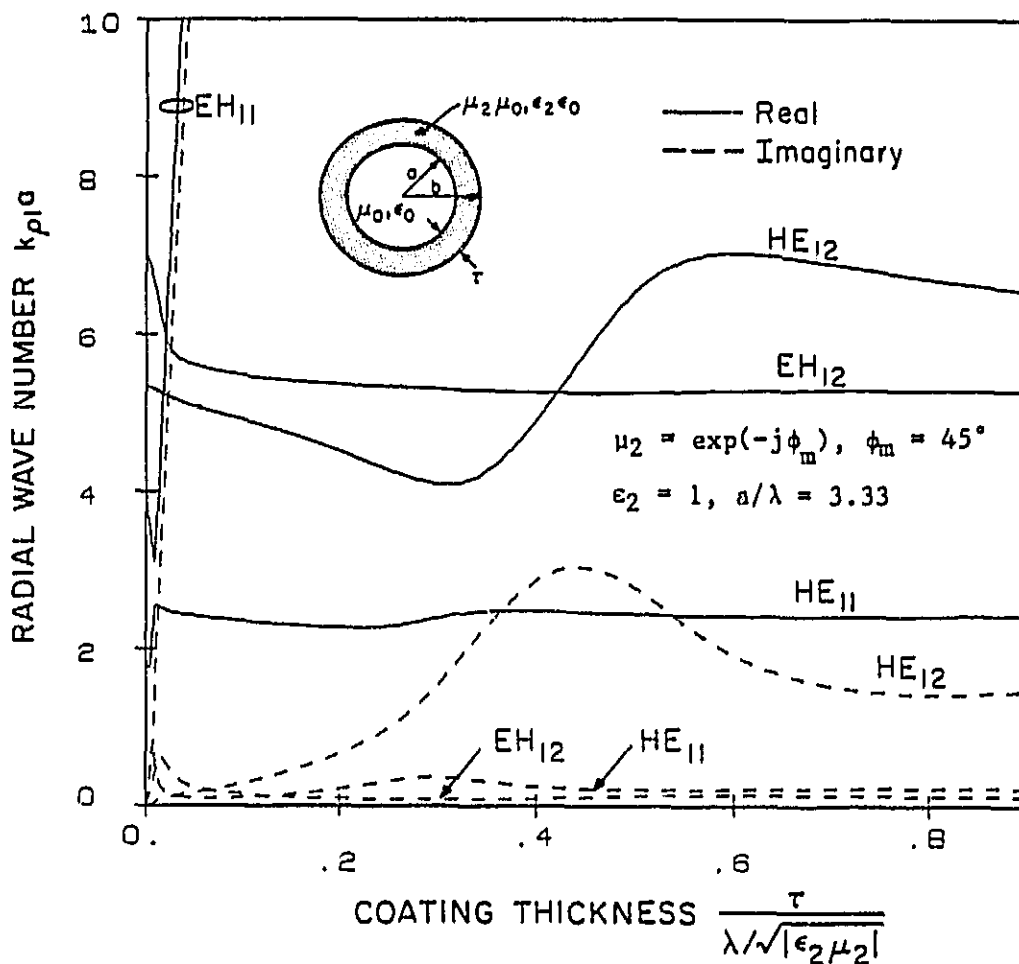


Figure 17. Radial wave numbers of the normal modes in a circular waveguide coated with a lossy magnetic material ( $\mu_2 = \exp(-j\phi_m)$ ,  $\phi_m = 45^\circ$ ,  $\epsilon_2 = 1$ ,  $a/\lambda = 3.33$ ).

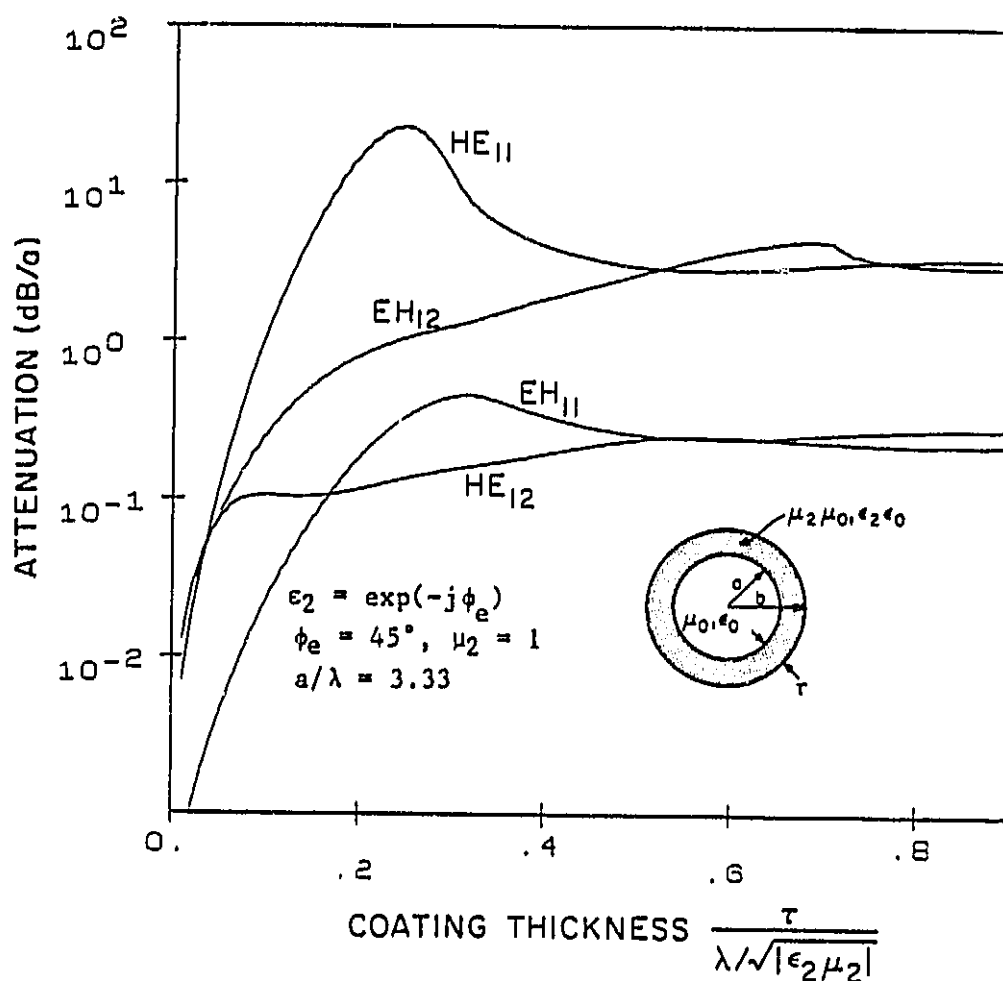


Figure 18. Attenuation constants of the normal modes in a circular waveguide coated with a lossy dielectric material ( $\epsilon_2 = \exp(-j\phi_e)$ ,  $\phi_e = 45^\circ$ ,  $\mu_2 = 1$ ,  $a/\lambda = 3.33$ ).

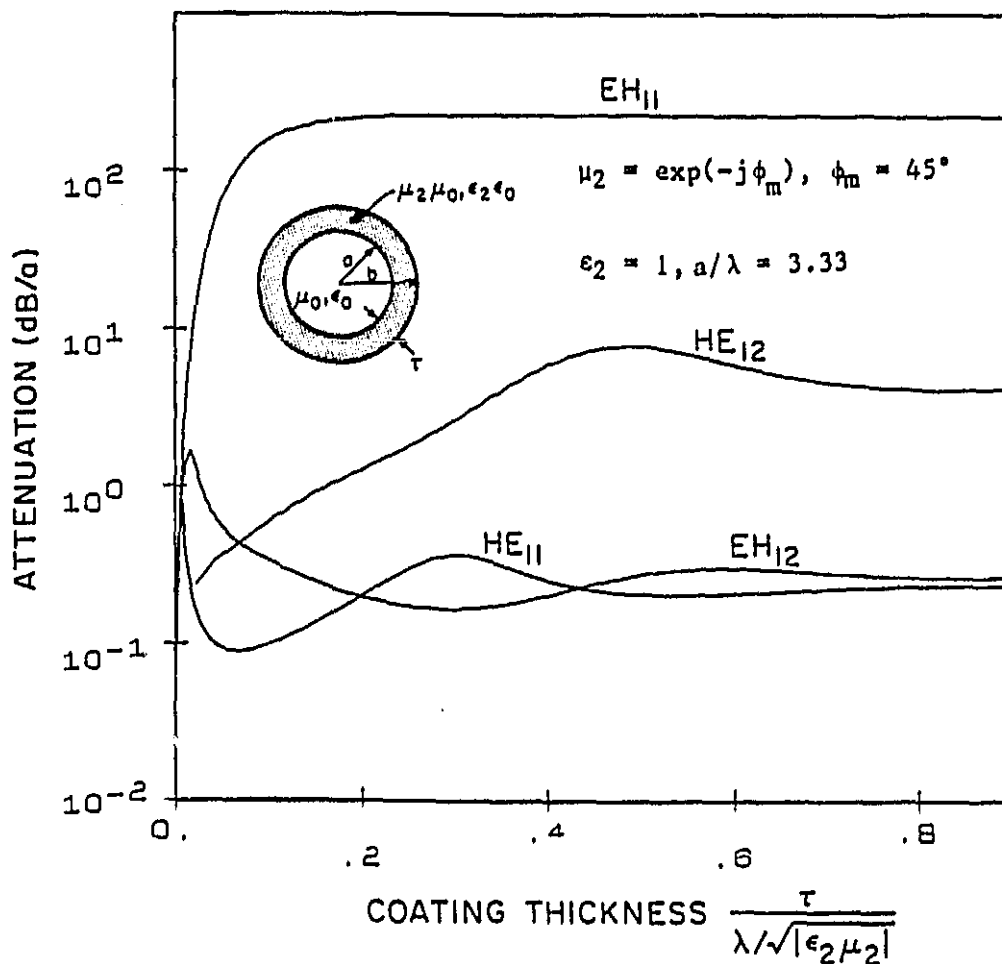


Figure 19. Attenuation constants of the normal modes in a circular waveguide coated with a lossy magnetic material ( $\mu_2 = \exp(-j\phi_m)$ ,  $\phi_m = 45^\circ$ ,  $\epsilon_2 = 1$ ,  $a/\lambda = 3.33$ ).

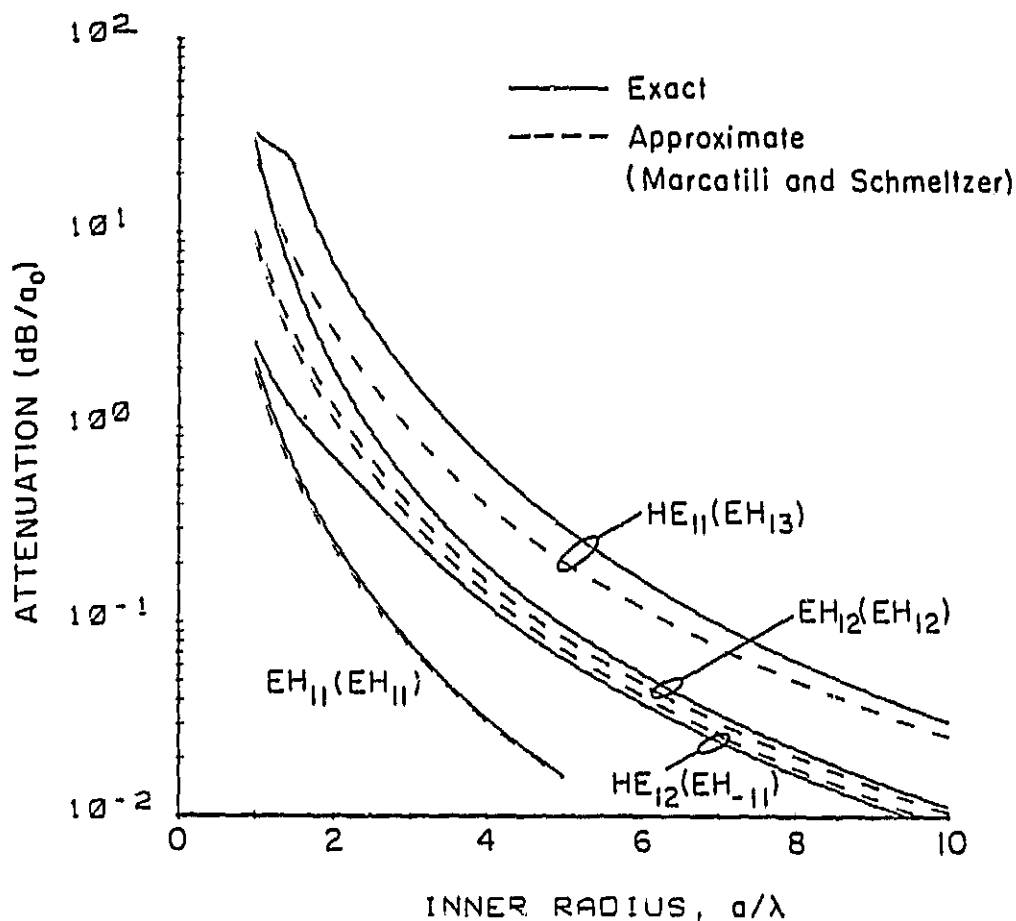


Figure 20. Attenuation constants of the normal modes as a function of the inner radius,  $a$ , with a fixed layer thickness ( $\tau = 0.949 \lambda / \sqrt{|\epsilon_2 \mu_2|}$ ) in a circular waveguide coated with a lossy dielectric material ( $\epsilon_2 = \exp(-j\phi_e)$ ,  $\phi_e = 45^\circ$ ,  $\mu_2 = 1$ ,  $a_0/\lambda = 3.33$ ). The mode names in the parentheses correspond to those in Marcatili and Schmeltzer's paper [5].

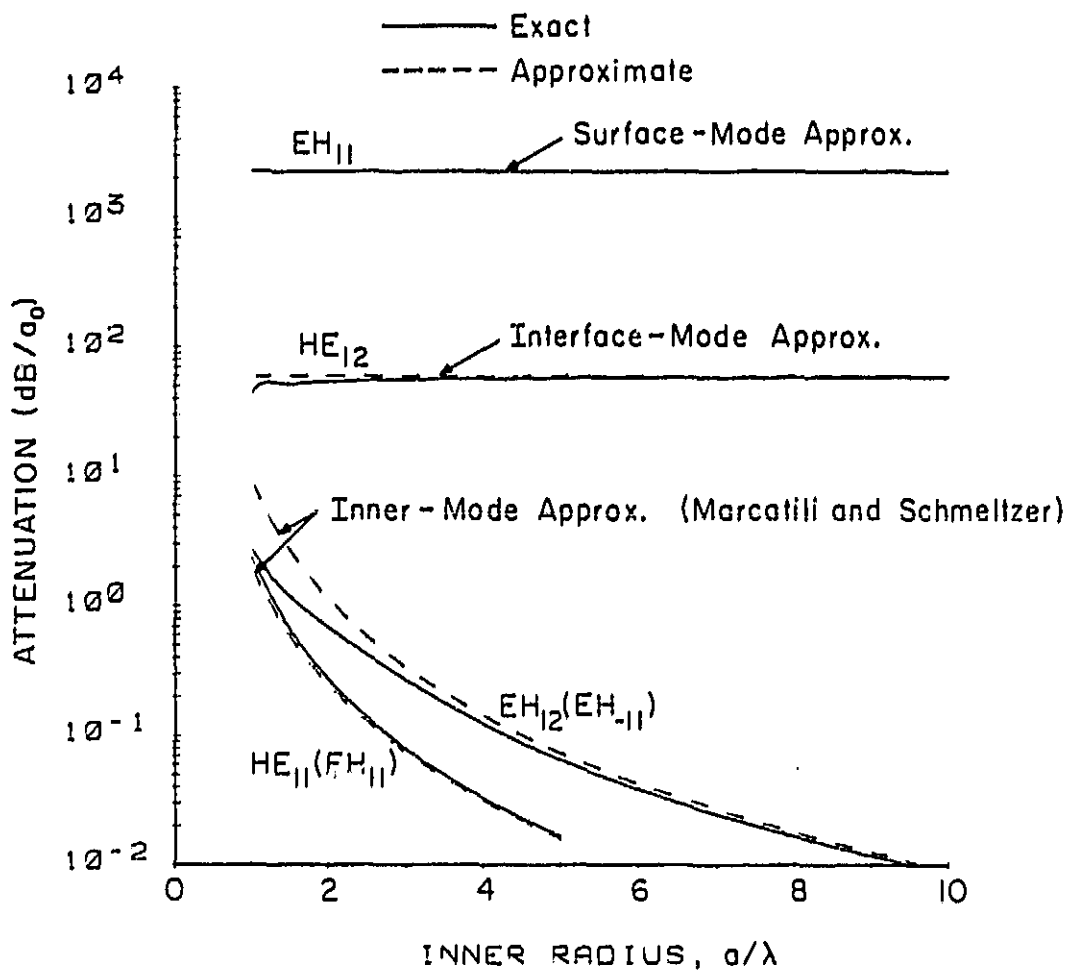


Figure 21. Attenuation constants of the normal modes as a function of the inner radius,  $a$ , with a fixed layer thickness ( $\tau = 0.949 \lambda / \sqrt{|\epsilon_2 \mu_2|}$ ) in a circular waveguide coated with a lossy magnetic material ( $\mu_2 = \exp(-j\phi_m)$ ,  $\phi_m = 45^\circ$ ,  $\epsilon_2 = 1$ ,  $a_0/\lambda = 3.33$ ). The mode names in the parentheses correspond to those in Marcatili and Schmeltzer's paper [5].